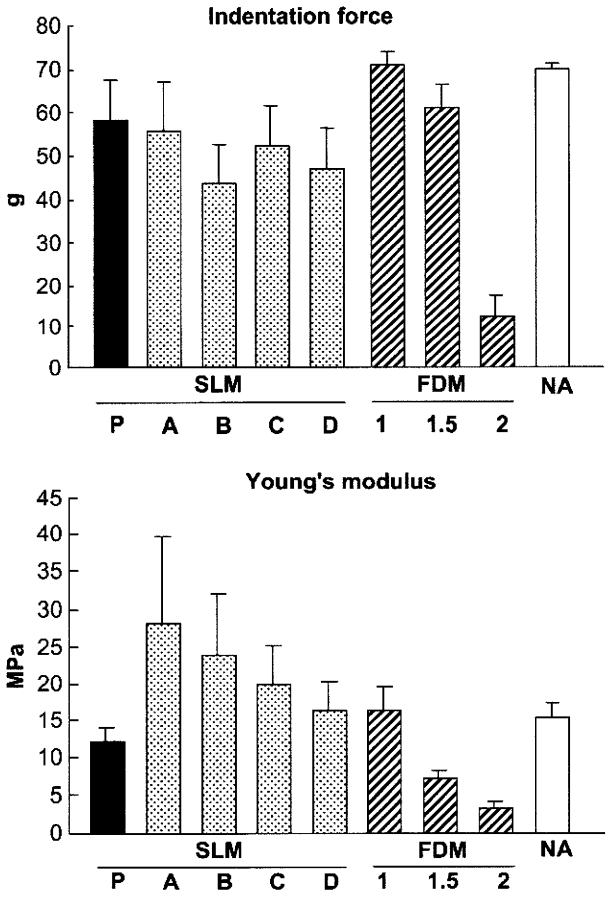

Fig. 2. Mechanical properties of porous scaffolds that had various structures. The indentation force and Young's modulus for each scaffold and human native articular cartilage (NA) were measured using a Venustron tactile sensor. All values are presented as mean plus standard deviation of 5 measurements per group.

hydrolysis because it contains less crystalline regions than PLLA [26]. In addition, the copolymers associated with the lactide are rapidly absorbed and would be smoothly replaced by the regenerated cartilage. We also examined the typical copolymers, poly-L-lactide-co-glycolide (PLGA) and chose PLGA(L) (LA:GA = 30:70, M_w 10^5) which is used in clinical applications as a bioabsorbable suture [27]. We also prepared a higher molecular weight PLGA(H) (LA:GA = 30:70, M_w 2×10^5). Moreover, we evaluated another copolymer, poly(L-lactide-co-e-caprolactone) (PLA/CL, M_w 2×10^5), which is also used as an absorbable surgical suture with a biodegradation time that ranged between two and six months. It is shorter than PLGA, but faster than PLLA [26]. We used PLA/CL with the copolymerization rate of 50:50, which was used for the clinical application of artificial blood vessels or artificial dura matter. Thus, we prepared five kinds of scaffolds consisting of PLLA, PLGA(L), PLGA(H), PLA/CL and PDLA, and evaluated the properties of the scaffolds and the tissue-engineered cartilage, as well as the degree of polymer biodegradation or tissue reaction in and around the tissue-engineered cartilage.

2. Materials and methods

2.1. Chemicals and antibodies

Dulbecco's Modified Eagle's Medium Nutrient Mixture F-12 HAM (DMEM/F-12), penicillin–streptomycin solution, human serum, and trypsin–EDTA solution were purchased from the Sigma Chemical Co. (St. Louis, MO, USA). Collagenase from *Clostridium histolyticum*, chloroform, and sucrose were purchased from Wako Pure Chemical Industries (Osaka, Japan). The other reagents included fibroblast growth factor-2 (FGF-2) (Kaken Pharmaceutical Co., Ltd., Tokyo, Japan), atelocollagen (Koken Co., Ltd., Tokyo, Japan), fibroblast growth factor-2 (FGF-2) (Kaken Pharmaceutical Co., Ltd., Tokyo, Japan), insulin (MP Biomedicals, Inc., Irvine, CA, USA), OCT compound (Miles, Elkhart, IN, USA), poly-L-lactide (PLLA, M_w: 300 kDa, Polysciences, Inc., Warrington, PA, USA), Histofine® 10% normal rabbit serum (Nichirei Biosciences, Inc., Tokyo, Japan), and antimouse F4/80 antigen rat monoclonal IgG2b (clone CI:A3-1, Biomedical AG, Augst, Switzerland).

2.2. Chondrocyte isolation and preparation

All procedures for the present experiments were approved by the Ethics Committee of the University of Tokyo Hospital (ethics permission #622). With 0.15% collagenase digestion, the human chondrocytes were isolated from the remnant auricular cartilage of microtia patients who underwent an operation at the University of Tokyo Hospital, with informed consent. The isolated chondrocytes were seeded in a 100 mm plastic tissue culture dish at a density of 6400 cells/cm^2 and cultured in the DMEM F/12 containing 5% human serum, 100 ng/mL FGF-2, and 5 μg/mL insulin with 100 mm/Collagen Type 1 Coated Dish (Iwaki brand Scitech Div. Agc Techno Co., Ltd., Chiba, Japan), in a 37 °C/5% CO_2 incubator [28,29]. The medium was changed two times per week. Passages were performed by treatment with trypsin–EDTA solution when the cells were approaching confluence.

2.3. Scaffold preparation

We prepared eight kinds of PLLA porous scaffolds with the dimensions of 8 mm × 8 mm × 3 mm, using two procedures. We first made the prototype porous scaffold (Fig. 1P). According to a previous paper [30], 0.8 g of the polymer was dissolved in 5 mL of chloroform, then sucrose (approximately 2.0 mm average particle size) was added to the mixture at a 1:20 ratio of PLLA as the porogen. The polymer–porogen mixture was placed in a 10 mm × 10 mm × 5 mm mold, and the chloroform was evaporated. Finally, the mixture was submerged in water for 45 min to dissolve the sucrose to produce the porous scaffolds. These scaffolds were dried overnight, then trimmed with a surgical knife (Fig. 1P). Besides the prototype, we used various porogens with different sizes at different mixing ratios in the SLM to uniquely make four kinds of scaffolds which possess structures with different pore sizes and porosities by the SLM (KRI, Kyoto, Japan, Fig. 1A–D). We used two different kinds of sucroses, the particle sizes of which were approximately 0.8 mm and 1.5 mm on average. The porogen was mixed at the ratio of 1 to 15 or 25. As the SLM method for the A scaffold, the particle size was 0.8 mm and the ratio was 1 to 15, while those of B were 0.8 mm and 1 to 25. Those of C were 1.5 mm and 1 to 15, while the D was 1.5 mm in particle size and 1:25 as the mixing ratio (Fig. 1A–D).

For the FDM, the 3-D modeling system was used for manufacturing scaffolds (Corefront Corporation, Tokyo, Japan). The 3-D modeling system produces the PLLA in the fused form (170 °C) through the deposition nozzle. The 3 kinds of specifically designed scaffolds were manufactured, with sizes of 8 mm × 8 mm × 3 mm, the width of the PLLA fibers was 1.0 mm and the aperture sizes (pore size) of the scaffolds were 1.0 mm, 1.5 mm and 2.0 mm, respectively (Fig. 1 FDM).

The average pore sizes were examined in the images from the scanning electronic microscope (SEM2460 N, Hitachi, Tokyo, Japan). To evaluate the average porosity of each scaffold, we measured the edges of the scaffold cubes and then calculated the volume (Vscaffold). We then weighted the scaffolds (Wscaffold), and the weight of the scaffolds was divided by the density of the polymer (1.25, ρ polymer) to obtain the volume of the polymer. We eventually divided the scaffold volume by the volume of the polymer to get the porosity. It was expressed by the following formula: Porosity (%) = (Vscaffold − Vpolymer)/Vscaffold × 100% = (Vscaffold − Wscaffold/ρ polymer)/Vscaffold × 100%.

We also prepared the porous biodegradable polymer scaffolds consisting of PDLA (M_w: 200 kDa), PLA/CL 50:50 (M_w: 200 kDa), and PLGA(L or H) (30:70, M_w: 100 or 200 kDa), which were produced by KRI, Inc.(Kyoto, Japan), by the SLM.

2.4. Mechanical properties of each scaffold

The indentation force and Young's modulus of each porous scaffold or native articular cartilage were measured using a Venustron tactile sensor (Axiom, Fukushima, Japan). Under computer control, the motor-driven sensor unit automatically presses down on the surface of the materials and provides an indentation force and a decrease in the resonant frequency. The resonant frequency of the sensor was set to 50 Hz, while the maximum depth of indentation was 1 mm. Young's modulus can be calculated by the indentation force and the decrease in the resonant frequency, based on the principles reported by Aoyagi and Yoshida [22]. Venus 42 software provided by the manufacturer was used for the calculation.

2.5. Retainment of medium and atelocollagen in the scaffolds

We examined the retainment of DMEM/F-12 or 1% atelocollagen in the scaffolds. We measured the volume (Vscaffold) and weight (Wscaffold) of the scaffolds. Next, we measured the weight after immersion into the medium: (Mscaffold) or atelocollagen: (Ascaffold). We subtracted the normal weight from the immersed weight, then divided by the volume of the scaffolds to get the retainment per 1 cm^3 of each scaffold. It was expressed by the following formula: Retainment (g/1 cm^3) = {(M/A) scaffold − Wscaffold}/(Vscaffold).

2.6. Preparation of tissue-engineered cartilage and the subcutaneous implantation into nude mice

The human auricular chondrocytes at the third passage were suspended in 1% atelocollagen solution at the cell density of $1 \times 10^{7-8}$ cells/mL. They were then put into various porous scaffolds and incubated in a 37 °C/5% CO_2 incubator for 2 h, leading to gelation. We then obtained the implant-type tissue-engineered cartilage. For the in vivo analyses, the constructs were subcutaneously transplanted in Bulb-c nude mice (6 weeks old, male) under Nembutal anesthesia. After 2 months, we harvested the samples also under Nembutal anesthesia. After photographing, each sample of tissue-engineered cartilage was divided into half. One half was quickly frozen by liquid nitrogen for biochemical measurement, while the other was fixed with 4% paraformaldehyde in 0.1 M phosphate buffer (pH 7.4) for 2 h at 4 °C for histological analyses.

2.7. Biochemical measurement of collagen types I (COL1) and II (COL2) and glycosaminoglycan (GAG)

Samples were minced by scissors and homogenized twice for 30 s each by a homogenizer (IKA®-T10 basic ULTRA-TURRAX® Staufen, Germany). These samples were dissolved in 10 mg/mL pepsin/0.05 M acetic acid at 4 °C for 48 h and then in 1 mg/mL pancreatic elastase/1 × TSB at 4 °C. Any cell debris and insoluble material were removed by centrifugation at 6000×g for 30 min. We then measured these conditioned samples.

COL1 and COL2 proteins were quantified by ELISA according to the protocol of the human Types I, II Collagen Detection Kit (Chondrex, Redmond, WA, USA). For the ELISA measurement, we diluted the supernatant at 1:100 with the dilution buffer. In the sample mixture, the collagen proteins were captured by polyclonal anti-human COL1 or COL2 antibodies and detected by the biotinylated counterparts and streptavidin peroxidase. OPD and H_2O_2 were added to the mixture, and sulfuric acid was then added after 30 min to stop the reaction. The spectrophotometric absorbance of the mixture was measured at a wavelength of 490 nm by a spectral photometer (ARVO™SX 1420 MULTI LABEL COUNTER, Perkin–Elmer™, Waltham, MA, USA).

We evaluated the GAG content using the Alcian blue-binding assay (Wieslab AB, Lund, Sweden), according to the supplier's protocol. GAG in the supernatant was precipitated in Alcian blue solution, and the sediments after centrifugation at 6000×g for 15 min were dissolved again in a 4 M GuHCl-33% propanol solution. The

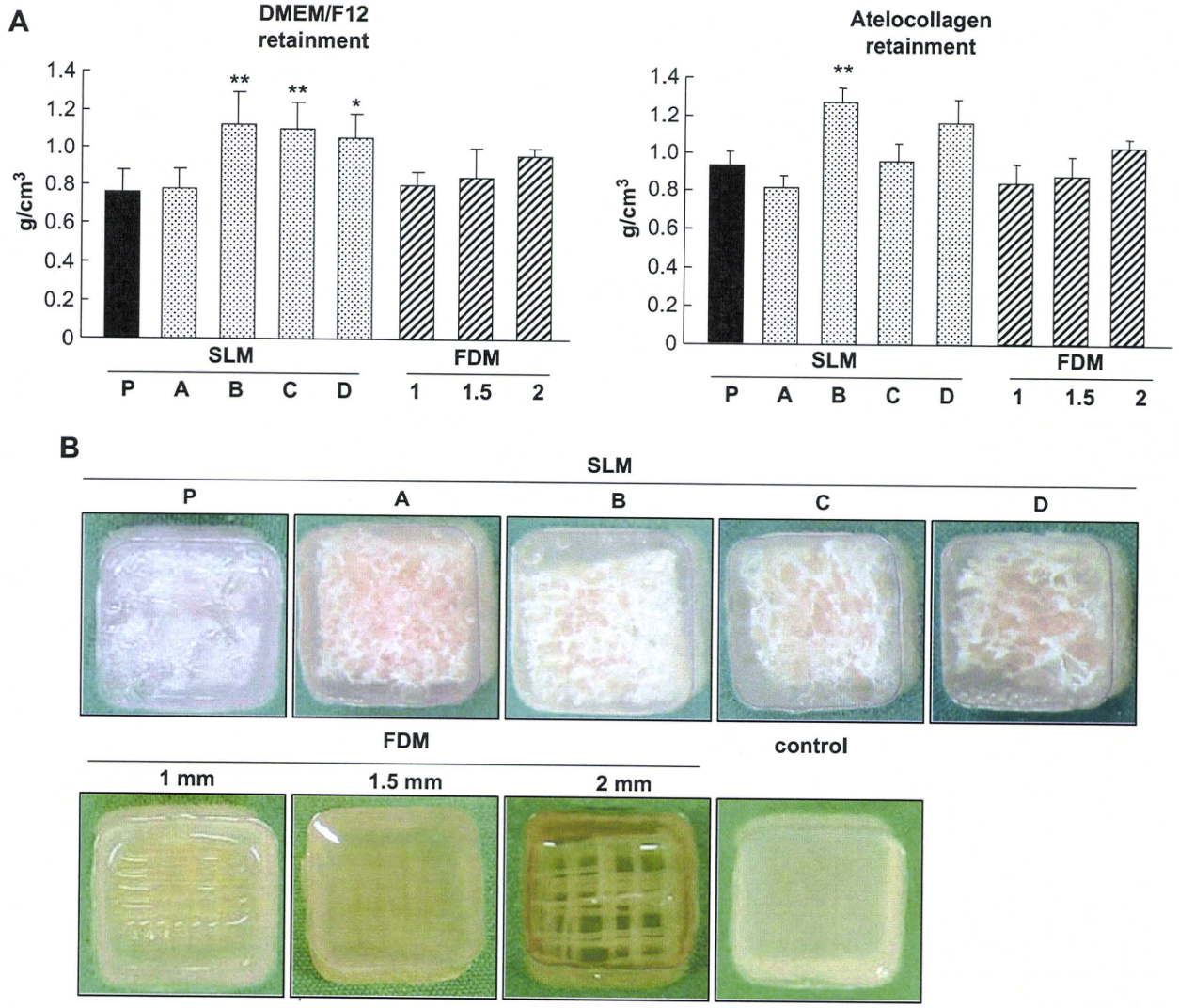

Fig. 3. The evaluation for the retained of medium and atelocollagen within the porous scaffolds that had various structures. A. Measurement of the retainment (weight per 1 cm^3 scaffold) in the cell culture medium (DMEM/F-12) or 1% atelocollagen gel in each scaffold. Both the medium and atelocollagen retainment of SLM B showed a significantly higher level than that of SLM P. All values are presented as mean plus standard deviation of 3 samples per group. Statistics were assessed using the Dunnett significance test (*$P < 0.05$, **$P < 0.01$ vs SLM P). B. Macroscopic findings of each scaffold after cell/gel mixture immersion. Mold sides = 10 × 10 mm.

spectrophotometric absorbance of the mixture was measured at a wavelength of 600 nm by a spectral photometer.

2.8. Histological and immunohistochemical analyses

The samples fixed with the paraformaldehyde were successively immersed in 10% sucrose in phosphate-buffered saline (PBS), 20% sucrose in PBS, and a 2:1 mixture of 20% sucrose of PBS and OCT compounds. The samples were rapidly frozen in liquid nitrogen, and were then cryosectioned at a thickness of 10 μm (CM1850-Kryostat, LEICA, Solms, Germany), stained with toluidine blue-O and observed by optical microscopy (Olympus DP 70, Tokyo, Japan).

We also examined the immunolocalizations of macrophages against the F4/80 antigen. The sections were immersed in methanol with 3% H_2O_2 buffer for 15 min to remove endogenous peroxidase and blocked with 10% normal rabbit serum for 10 min. After blocking, the primary antibodies against F4/80 were placed onto the sections and incubated for 1 h at 37 °C. The signals were detected by Biotinated anti-Rat IgG (H + L) made in a rabbit Vectastain® Elite® ABC Kit Pk-6100 (Vector Laboratories, Inc., Burlingame, CA, USA) and DAB Substrate Kit for Peroxidase sk-4100 (Vector Laboratories, Inc.). Finally, hematoxylin was used for counterstaining. For morphometrical analysis of the macrophage numbers, we counted the numbers of the F4/80 positive cells per 1 cm^2 in three images from different sections of each group.

3. Results

3.1. Morphology and mechanical properties of PLLA scaffolds with various structures

First of all, we evaluated the structure of porous scaffolds consisting of PLLA. For the actual measurement, the average pore sizes and the average porosities of the SLM scaffolds were: P, 1.0 mm and 80%; A, 0.3/90%; B, 0.3/95%; C, 0.6/90%; D, 0.6/95% (Fig. 1, SLM). On the FDM, the aperture sizes (pore sizes) of the scaffolds were set to 1.0 mm, 1.5 mm and 2.0 mm, for which the porosities were 85%, 88% and 90%, respectively (Fig. 1, FDM).

When we measured the mechanical properties of each scaffold using the Venustron tactile sensor, the scaffold with the higher porosity tended to show a lower indentation force when compared among those made by the same methods (Fig. 2, indentation force). Especially, the FDM scaffold with the 2.0 mm in aperture (FDM 2) had a decreased indentation force, showing approximately one seventh of that for the 1.0 mm aperture (FDM 1), which was almost equivalent to the native cartilage (Fig. 2, indentation force). The Young's modulus was lower in the scaffolds with the high pore sizes, for either manufacturing method (Fig. 2, Young's modulus). From a comparison among the scaffolds with the same porosity, Young's modulus seemed to decrease in the scaffolds with the larger pore sizes, as seen in the SLM scaffolds of C and D (Fig. 2, Young's modulus). The mechanical properties of SLM A, SLM B and FDM 1 had the same level as those of the native cartilage (Fig. 2, NA).

3.2. Cell–scaffold interaction study for PLLA scaffolds with various structures

To examine the cell–scaffold interaction, we measured the retainment (gram per 1 cm^3 scaffold) of the cell culture medium (DMEM/F-12) or 1% atelocollagen gel, either of which was mixed with chondrocytes when administered into the scaffolds. The retainment of both DMEM/F-12 and atelocollagen tended to increase in the scaffolds with the higher pore sizes and higher porosities (Fig. 3A). The DMEM/F-12 retainment in the SLM scaffolds of B, C and D was significantly greater than prototype (Fig. 3A, DMEM/F-12 retainment). The atelocollagen retainment of SLM B also showed a significantly higher level than that of SLM P (Fig. 3A, atelocollagen retainment). As observed in the macrographic findings (Fig. 3B), the atelocollagen permeation was easily visible in the FDM scaffolds. The atelocollagen also seemed to sufficiently permeate the SLM scaffolds in spite of the complex structures.

3.3. Cartilage properties of tissue-engineered constructs using PLLA scaffolds with various structures

To examine the cartilage properties of the tissue-engineered constructs using these scaffolds, we suspended the chondrocytes in atelocollagen and put them into each porous scaffold (Fig. 3B). They

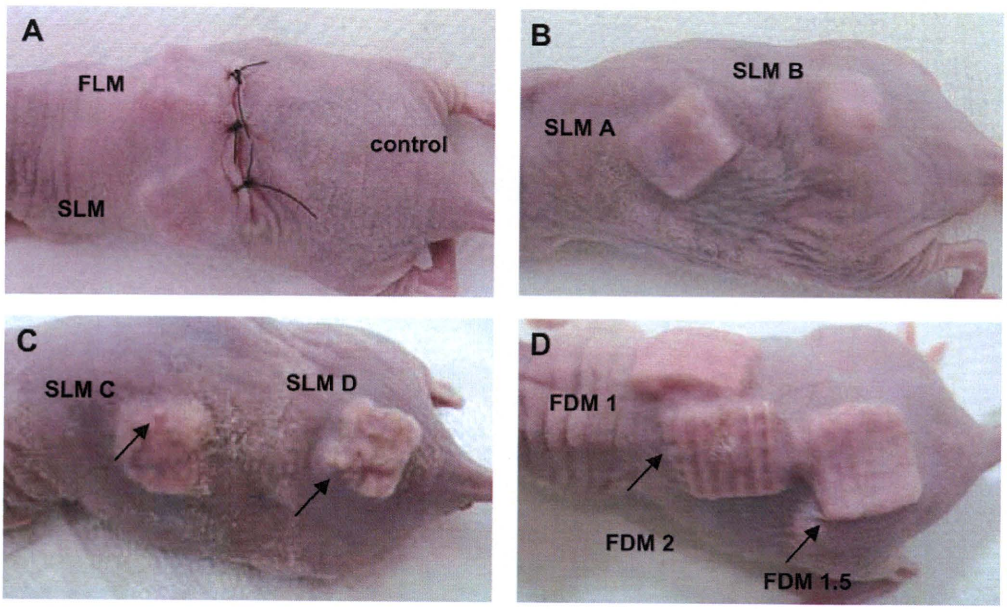

Fig. 4. Gross appearance of tissue-engineered constructs subcutaneously transplanted into the backs of nude mice. The constructs using porous scaffolds (8 × 8 × 3 mm) that had various structures were administered with the chondrocytes/atelocollagen mixture at the cell density of 1 × 10^7 cells/mL, and were subcutaneously transplanted into the backs of nude mice. A. Immediately after transplantation. The constructs using the scaffolds of SLM and FDM were noted, although no cell/atelocollagen mixture (control) was found through the skin. B–D. At 2 months in vivo, irregular shapes reflecting the contour of SLM C, SLM D, FDM 1.5 and FDM 2 were visible through the skins (arrows).

were then subcutaneously transplanted into the backs of nude mice (Fig. 4). All of the porous scaffolds could maintain their shapes expect in the control, in which the mixture of the chondrocytes and atelocollagen was transplanted without porous scaffolds (Fig. 4A). Immediately after the transplantation, the control hardly maintained their 3-D shapes, and we could not find it through the skin (Fig. 4A, control). At 2 months after transplantation, the surface of the skins covering the construct of SLM A and SLM B was smooth (Fig. 4B), but irregular shapes reflecting the contour of SLM C and SLM D were visible through the skins (Fig. 4C, arrows). The PLLA lattice structures of FDM 1.5 and FDM 2 also protruded through the skin (Fig. 4D, arrows). At 2 months, we removed the tissue-engineered constructs using each porous scaffold from the nude mice, and macroscopically and histologically observed the constructs. All of them, except for the control could maintain their 3-D shapes (Fig. 5, macro), although the control, which did not use any porous scaffolds, shrank in size. Among them, the construct of SLM B appeared whitish and smooth on its surfaces (Fig. 5, macro).

All the histological findings of the engineered tissues using the porous scaffolds showed some metachromatic areas after toluidine blue staining, suggesting the accumulation of proteoglycan that specifically occurs in the cartilage matrix. Especially, abundant metachromasia was observed in both SLM B and FDM 1.5 (Fig. 5, histology). Although control, which did not use any porous scaffolds, shrank in size, it also showed the dense metachromasia in such a small area (Fig. 5, histology).

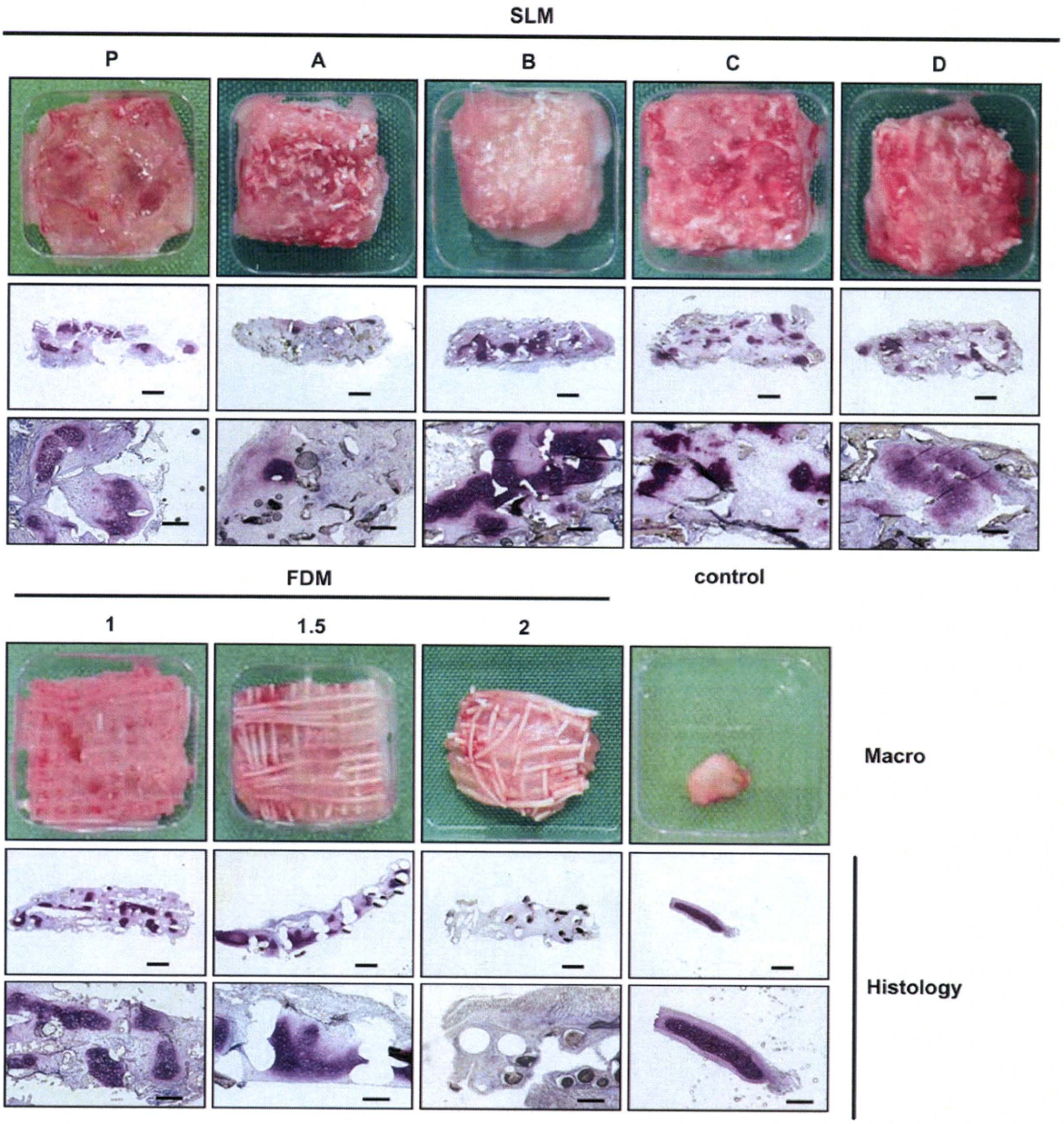

Fig. 5. Macroscopical and histological images of tissue-engineered constructs using porous scaffolds that had various structures. The constructs (8 × 8 × 3 mm) were administered with the chondrocytes/atelocollagen mixture at the cell density of 1×10^7 cells/mL, and were subcutaneously transplanted into the backs of nude mice. The constructs were harvested at 2 months after transplantation. Histological sections were stained with toluidine blue. Top, macroscopical images (macro, mold sizes = 10 mm). Middle (bar = 1 mm), bottom (500 μm).

Based on the biochemical measurements of the tissue-engineered cartilage using each scaffold, the COL1 contents showed no significant differences (Fig. 6, COL1). While the SLM B or the FDM 1.5 showed elevated levels of COL2 (Fig. 6, COL2), all four types of the SLMs including SLM B and FDM 1.5 showed significant increases in the GAG accumulation, compared with SLM P (Fig. 6, GAG), which implied a favorable cartilage regeneration in SLM B and FDM 1.5.

3.4. Cartilage properties of tissue-engineered constructs using the scaffolds with various compositions

Because the PLLA scaffold with the porosity of 95% and pore size of 0.3 mm made by the SLM effectively retained the cell/atelocollagen mixture in the scaffolds and indicated a fair cartilage regeneration, as shown above, we regarded it as the optimal structure, and compared the tissue-engineered cartilage using the scaffolds with the same structure, but consisting of PLLA, PLGA(L), PLGA(H), PLA/CL and PDLA. The indentation force and the Young's modulus of each scaffold were ranged between 20 and 50 g and 15–25 MPa, respectively, indicating that there was no extreme deviation from the values of PLLA. The retainment of DMEM/F-12 and 1% atelocollagen within each scaffold was also the same with that of PLLA.

The tissue-engineered cartilage constructs with the chondrocytes/atelocollagen mixture were subcutaneously transplanted in nude mice (Fig. 7). At 2 months, we could clearly observe the original 3-D shapes in all of the porous scaffolds. Neither constructs apparently protruded through the skin (Fig. 7, skin surface). When we harvested each tissue-engineered cartilage, they showed a smoother surface. The polymer remnants were hardly observed in the macroscopic findings. Although the colors in the constructs using the PLGA(L) and the PLGA(H) scaffolds were prominently whitish, the edges of the PLGA constructs became dull (Fig. 7, macro). In the histological findings, all of them showed a dense accumulation of metachromatic areas that were toluidine blue stained. The ratio of the metachromatic area in the PLGA(L) construct seemingly increased when compared to the other constructs. From the observations under higher magnification, the remnants of the polymers were found not in the PLGA constructs, but in the PLLA, PLA/CL, and PDLA constructs (Fig. 7, histology). The biochemical measurement of the COL1 content was significantly higher in the PLGA(H) than in the others (Fig. 8, COL1). Among all the constructs, both the COL2 and GAG contents were significantly higher in the PLLA or PLGA constructs when compared to those of PLA/CL and PDLA (Fig. 8, COL2 and GAG).

3.5. Evaluation of the tissue reaction in the tissue-engineered cartilage constructs

For determining the reasons why there are some differences in the cartilage regeneration of the constructs using each scaffold, we focused on the tissue reaction in the tissue-engineered cartilage, which may influence the viability or activity of the chondrocytes. We investigated the immunolocalizations of the macrophages which constitute the main part of tissue reaction [31]. As the result, macrophages were localized in the non-cartilaginous areas, especially the areas on and around the polymers (Fig. 9, arrows). We found dense localization of the macrophages in the constructs using PLA/CL and PDLA (Fig. 9D and E). While the polymer

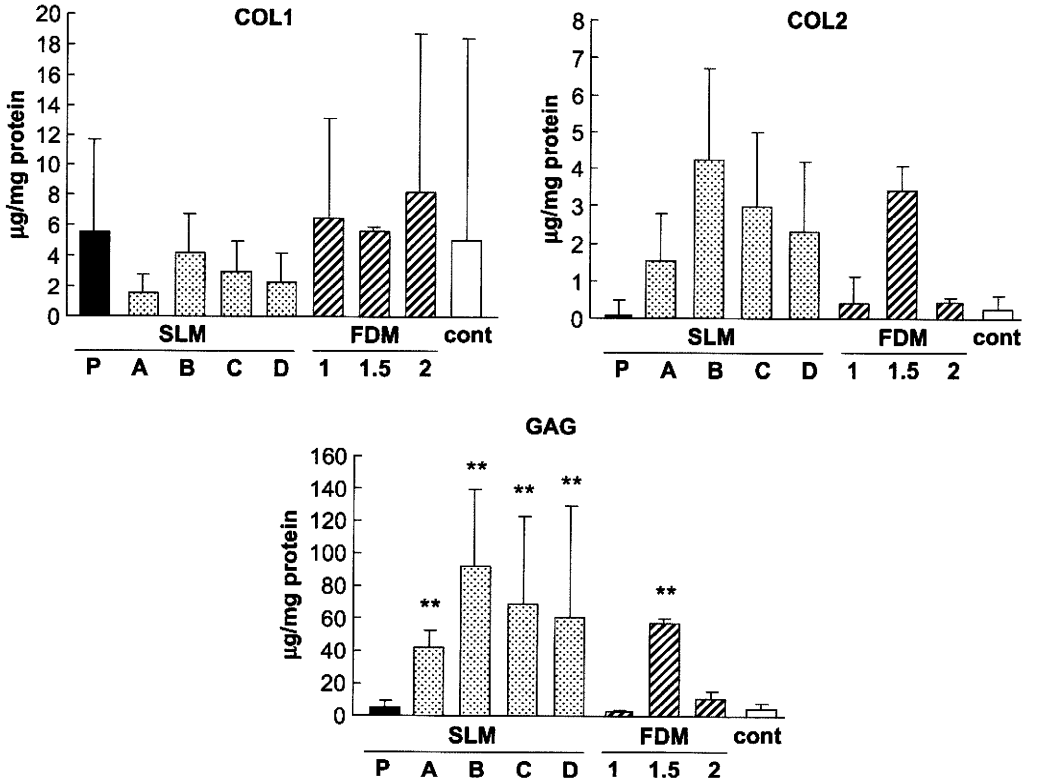

Fig. 6. The biochemical measurements of tissue-engineered constructs using porous scaffolds that had various structures. The constructs (8 × 8 × 3 mm) were administered with the chondrocytes/atelocollagen mixture at the cell density of 1×10^7 cells/mL, were subcutaneously transplanted into the backs of nude mice, and were harvested at 2 months after transplantation. The SLM B or the FDM 1.5 showed the elevated level of COL2 or GAG. cont: Control. All values are presented as mean plus standard deviation of 3 samples per group. Statistics were assessed using the Dunnett significance test (**$P < 0.01$ vs SLM P).

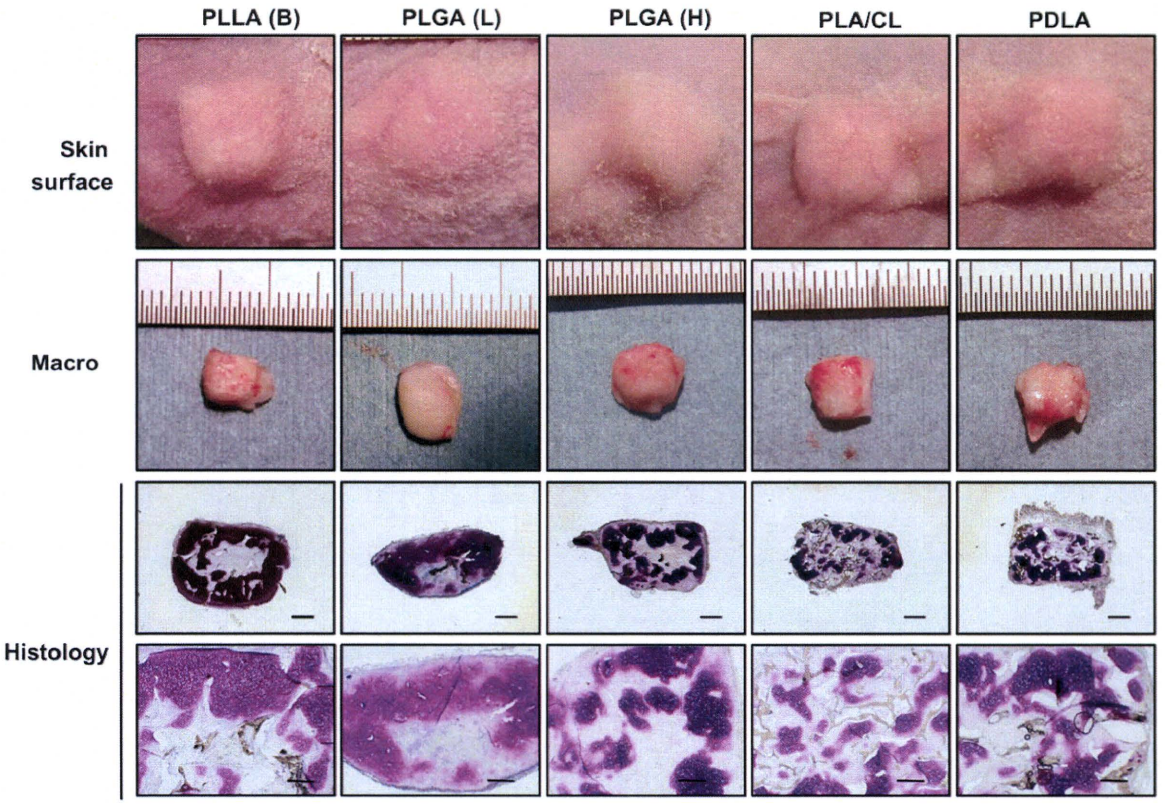

Fig. 7. Macroscopic and histological images of tissue-engineered constructs made of the porous scaffolds consisting of various biodegradable polymers with the chondrocytes/atelocollagen mixture at the cell density of 1×10^8 cells/mL. The constructs ($4 \times 4 \times 3$ mm) were transplanted into the backs of nude mice. At 2 months in vivo, the skin surface was smooth in all the polymers. Based on the toluidine blue histological findings, the metachromatic areas were more expansive than those in the experiment using 1×10^7 cells/mL. Macro, and macroscopic images (bar = 2 mm); histology, bar = 1 mm (lower magnification) and 500 μm (higher magnification).

remnants were hardly seen in the constructs of PLGA, less accumulation of the macrophages was also detected (Fig. 9B and C). We morphometrically assessed the number of macrophages in all the constructs, revealing that they had significantly decreased in the constructs of PLGA for both molecular weights, when compared to those of the other polymers (Fig. 9F).

4. Discussion

In the present study, we examined the properties of the tissue-engineered cartilage using the porous scaffolds of PLLA as the typical biodegradable polymer, with various kinds of morphologies, pore sizes and porosities, and determined the structure suitable for the scaffold that effectively retains the cells/hydrogel mixture and enables fair cartilage regeneration.

The SLM has some advantages such that it does not need any specific equipment or that the cost could be reasonable. Moreover, if the 3-D shapes of the scaffolds were constant, mass production of the scaffolds could be facilitated. However, the equipment which had been used for manufacturing the FDM in the present study could not manage the diameter of fiber diameters less than 1 mm because of the limitation in the viscosity of polymers and the accuracy of the nozzle handling. The thick diameter of the fibers in the scaffold of the FDM interferes the increase in porosity. The volume ratio of polymers in the regenerative tissue becomes higher as the porosity decreases. In other words, the occupancy of the chondrocytes/atelocollagen mixture in the construct, which determines the volume of the regenerative tissue, is proportional to the porosity of the scaffold. For example, when the porosity is 80%, the cell-containing component occupies 80% of the total volume. The remaining 20% corresponds to the biodegradable polymers, implying that the shrinkage of 20% by the construct might occur when the polymer is biodegraded in the body. Thus, we would like to make a scaffold which has as high a porosity as possible. However, for the FDM, the high porosity was a hard task because their fiber size was set up 1 mm in the machine we had used. If the FDM scaffold with a 1 mm fiber size would generate than a 90% porosity, we should set the interval to over 1.5 mm. Actually, the abundant observation of metachromasia in the histology and the dense accumulation of COL2 and GAG in biochemical measurement were noted for the tissue-engineered cartilage using the FDM scaffold of 1.5 (Figs. 5 and 6). However, when the pores (the interval) were over 1.5 mm in size in the scaffolds, the tissue-engineered cartilage may not sufficiently retain the chondrocytes/atelocollagen mixture under in vivo conditions. In this case, the gel materials of the chondrocytes/atelocollagen mixture shrunk, while the lattice of the scaffold appeared from the tissue-engineered cartilage and extruded the skin (Fig. 4D). The reason why the production of cartilaginous matrices decreased in the FDM 2.0 might be due to the fact that the pores were too large to retain the chondrocytes/atelocollagen mixture. Thus, in the present study, we could not find a suitable structure among the FDM scaffolds.

We also evaluated the compositions of the porous polymer scaffolds with the porosity of 95% and pore size of 0.3 mm made by the sugar leaching method, as the ideal structure. Among the polymers, PLGA, which is rapidly biodegraded, or PLLA with a slow biodegradation rate, showed the formation of the tissue-engineered cartilage by a significant cartilage matrix synthesis. When

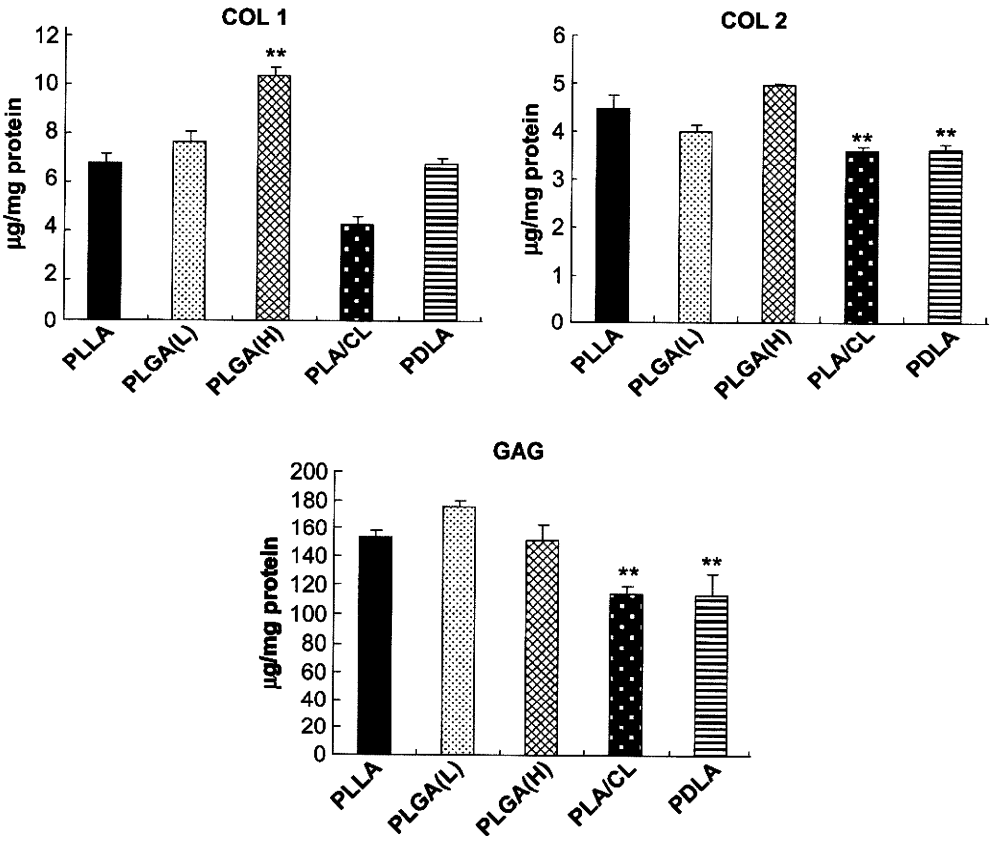

Fig. 8. The biochemical measurements of tissue-engineered constructs made of the porous scaffolds consisting of various biodegradable polymers with the chondrocytes/atelocollagen mixture at the cell density of 1×10^8 cells/mL. Both the COL2 and GAG contents were significantly higher in the PLLA or PLGA constructs, than those of PLA/CL and PDLA. All values are presented as mean plus standard deviation of 3 samples per group. Statistics were assessed using the Dunnett significance test (**$P < 0.01$ vs PLLA).

we observed the histological findings of the PLGA-based engineered tissues two months after the transplantation in nude mice, we could hardly find any remnant of the PLGA scaffolds even for the 2×10^5 molecular weight (Fig. 7), indicating that the polymer was readily degraded. The macroscopic findings also showed that the tissue-engineered cartilage using the PLGA scaffolds was whitish and smooth like a native cartilage (Fig. 7). The immunohistochemical findings disclosed that the localization of the macrophages was sparse, implying the suppression of a severe tissue reaction in the PLGA-based cartilage (Fig. 9F).

The macrophages are known to secrete the inflammatory cytokine of TNFα, IL-1β, and PGE_2 [32,33]. In joints suffering from the local inflammation of rheumatoid arthritis, these inflammatory cytokines make the synovial cells significantly produce catabolic enzymes including matrix metalloproteinases (MMPs), which degrade the cartilage matrix consisting of proteoglycan and COL2 [34]. The inflammatory cytokines also induce cyclooxygenase-2 (COX-2) or inducible nitric oxide synthase (iNOS), either of which prevents the production of proteoglycan and COL2 in the chondrocytes [35]. The PLGA scaffold in the tissue-engineered cartilage was rapidly degraded, which may suppress the increase in the macrophage numbers. This was why the inflammatory cytokines and subsequent tissue reaction were prohibited, leading to the higher quality tissue-engineered cartilage.

The biodegradation of PLA/CL or PDLA occurs more slowly than that of PLGA. The tissue-engineered cartilage using PLA/CL and PDLA contained the dense localization of macrophages and showed less accumulation of cartilage matrices than that in PLGA. The remaining metabolic products that induce the migration of macrophages over a long term may prolong the tissue reaction. Especially, the metabolites of PLA/CL, the caprolactone monomers, seem to have a cell toxicity [36]. They also work as a harmful factor for cartilage regeneration. In contrast, PLLA, the biodegradation of which was the slowest among those polymers, showed a comparatively fair regeneration. The reason for the local concentration of metabolic products being rather low is due to the slow progression of the biodegradation, which suppressed the migration of the macrophages and tissue reactions.

Based on these results, the PLGA scaffolds may be suitable for the implant-type tissue-engineered cartilage. Although a fair cartilage regeneration was observed in the tissue-engineered cartilage using PLGA, some constructs that had originally been block-shaped became edging off and shrunk. This phenomenon may be caused by the rapid degradation of the porous PLGA scaffolds before the sufficient accumulation of the cartilage matrices which the transplanted chondrocytes produce. The ideal absorption of biodegradable polymers should be synchronized with the cartilage regeneration. In our present method, it takes approximately two months for maturation of the tissue-engineered cartilage in vivo (Fig. 7). We need further experiments to establish the ideal scaffolds by optimization of the biodegradability in the polymers. Additionally, we should accumulate the knowledge and experience of postoperative time-dependent changes for the 3-D shapes of the tissue-engineered cartilage, not only in the immunocompromised animals, such as nude mice, but also in the rodents or the large-sized animals with normal immune systems.

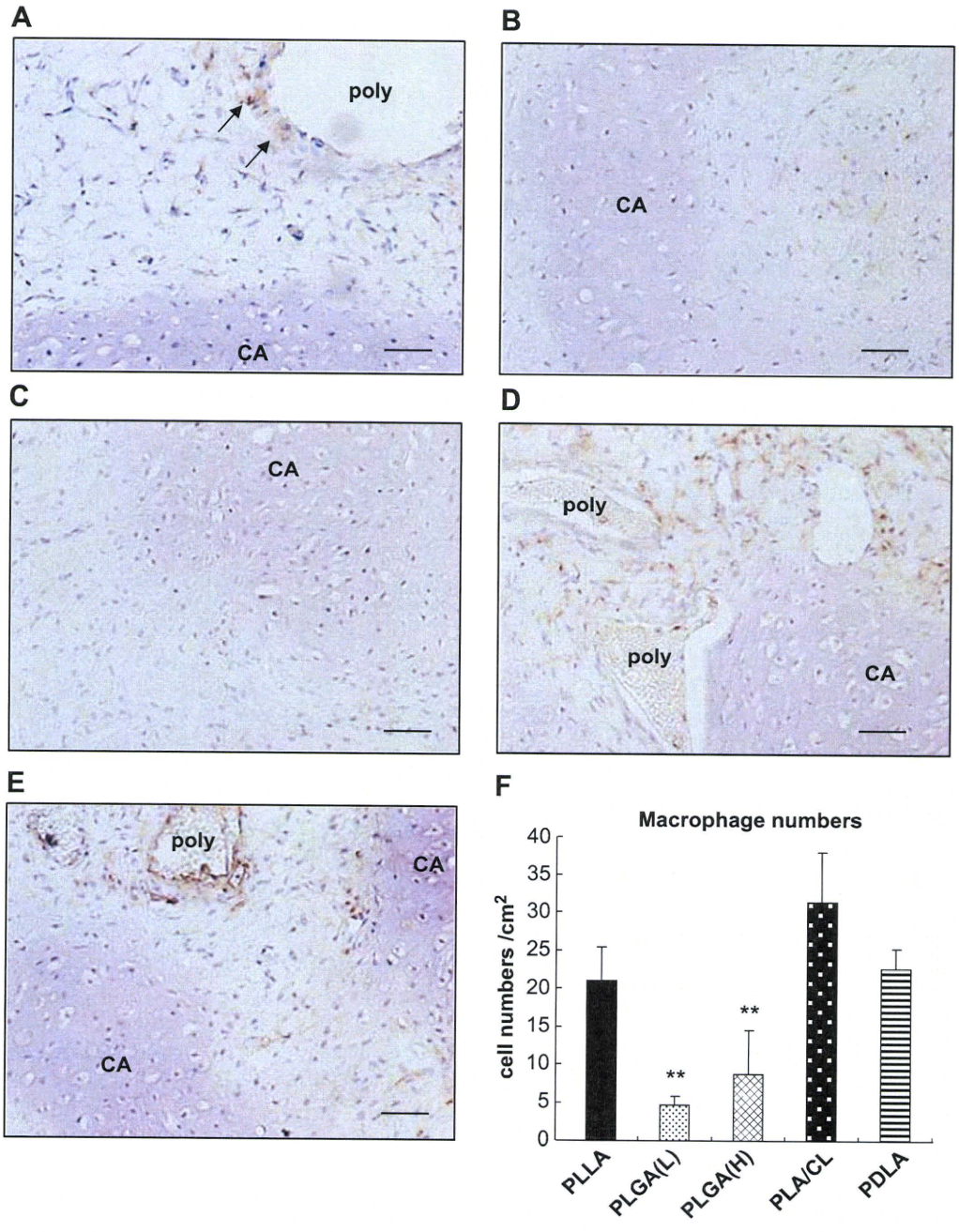

Fig. 9. The immunohistochemical localization of the macrophages in the constructs using the scaffold consisting of various polymers. A–E: The immunohistochemical localization of the macrophages by F4/80. There were polymer remnants (poly) in PLLA (A), PLA/CL (D) and PDLA (E), in which the localization of the macrophages accumulated around the remnants, but not in the regenerative cartilage (CA). Especially, multinucleated cells (arrows) were noted around the remnants. B: PLGA (L), C: PLGA (H). Bar = 100 μm. F: The number of macrophages in all constructs of each scaffold. All values are presented as mean plus standard deviation of 3 samples per group. Statistics were assessed using the Dunnett significance test (**$P < 0.01$ vs PLLA).

5. Conclusions

The structure optimal for the porous scaffold in combination with the atelocollagen was regarded to be that with the porosity of 95% and pore size of 0.3 mm made by the sugar leaching method, which effectively kept the chondrocytes/atelocollagen mixture in the scaffolds and indicated a fair cartilage regeneration. Regarding the comparison among PLLA, PDLA, PLA/CL and PLGA, PLGA and PLLA were superior to the others, when the tissue-engineered cartilage using each polymer was transplanted in nude mice. Although either of polymers has been currently recommended for the scaffold of cartilage, the polymer for which biodegradation is exactly synchronized to the cartilage regeneration would improve the quality of the tissue-engineered cartilage.

Acknowledgements

We appreciate Mr. Masahiro Sato and Mr. Fengzhe Jin (KRI, Kyoto, Japan) or Mr. Kazuo Hatae (Corefront, Tokyo, Japan) for their scientific advices on scaffold production. We also thank Mr. Motoki

Yagi for technical support. This work was supported by Grants-in-Aid for Scientific Research from the Ministry of Education, Culture, Sports, Science and Technology of Japan (MEXT, No. 21390532, 21592569 and 21659462), and Research and Development Programs for Three-dimensional Complex Organ Structures from the New Energy and Industrial Technology Development Organization and for Resolving Critical Issues from Special Coordination Funds for Promoting Science and Technology (SCF) commissioned by MEXT.

References

[1] Marlovits S, Zeller P, Singer P, Resinger C, Vecsei V. Cartilage repair: generations of autologous chondrocyte transplantation. Eur J Radiol 2006;57:24–31.
[2] Caldamone AA, Diamond DA. Long-term results of the endoscopic correction of vesicoureteral reflux in children using autologous chondrocytes. J Urol 2001;165:2224–7.
[3] Uchio Y, Ochi M, Matsusaki M, Kurioka H, Katsube K. Human chondrocyte proliferation and matrix synthesis cultured in atelocollagen gel. J Biomed Mater Res 2000;50:138–43.
[4] Benya PD, Shaffer JD. Dedifferentiated chondrocytes reexpress the differentiated collagen phenotype when cultured in agarose gels. Cell 1982;30:215–24.
[5] Malemud CJ, Stevenson S, Mehraban F, Papay RS, Purchio AF, Goldberg VM. The proteoglycan synthesis repertoire of rabbit chondrocytes maintained in type II collagen gels. Osteoarthritis Cartilage 1994;2:29–41.
[6] Gerard C, Catuogno C, Amargier-Huin C, Grossin L, Hubert P, Gillet P, et al. The effect of alginate, hyaluronate and hyaluronate derivatives biomaterials on synthesis of non-articular chondrocyte extracellular matrix. J Mater Sci Mater Med 2005;16:541–51.
[7] Ushida T, Furukawa K, Toita K, Tateishi T. Three-dimensional seeding of chondrocytes encapsulated in collagen gel into PLLA scaffolds. Cell Transplant 2002;11:489–94.
[8] Hutmacher DW, Ng KW, Kaps C, Sittinger M, Klaring S. Elastic cartilage engineering using novel scaffold architectures in combination with a biomimetic cell carrier. Biomaterials 2003;24:4445–58.
[9] Hannouche D, Terai H, Fuchs JR, Terada S, Zand S, Nasseri BA, et al. Engineering of implantable cartilaginous structures from bone marrow-derived mesenchymal stem cells. Tissue Eng 2007;13:87–99.
[10] Yamaoka H, Tanaka Y, Nishizawa S, Asawa Y, Takato T, Hoshi K. The application of atelocollagen gel in combination with porous scaffolds for cartilage tissue engineering and its suitable conditions. J Biomed Mater Res A 2009;93:123–32.
[11] Sakai D, Mochida J, Yamamoto Y, Nomura T, Okuma M, Nishimura K, et al. Transplantation of mesenchymal stem cells embedded in atelocollagen gel to the intervertebral disc: a potential therapeutic model for disc degeneration. Biomaterials 2003;24:3531–41.
[12] Yamaoka H, Asato H, Ogasawara T, Nishizawa S, Takahashi T, Nakatsuka T, et al. Cartilage tissue engineering using human auricular chondrocytes embedded in different hydrogel materials. J Biomed Mater Res A 2006;78:1–11.
[13] Chou CH, Cheng WT, Kuo TF, Sun JS, Lin FH, Tsai JC. Fibrin glue mixed with gelatin/hyaluronic acid/chondroitin-6-sulfate tri-copolymer for articular cartilage tissue engineering: the results of real-time polymerase chain reaction. J Biomed Mater Res A 2007;82:757–67.
[14] Shangkai C, Naohide T, Koji Y, Yasuji H, Masaaki N, Tomohiro T, et al. Transplantation of allogeneic chondrocytes cultured in fibroin sponge and stirring chamber to promote cartilage regeneration. Tissue Eng 2007;13:483–92.
[15] Girotto D, Urbani S, Brun P, Renier D, Barbucci R, Abatangelo G. Tissue-specific gene expression in chondrocytes grown on three-dimensional hyaluronic acid scaffolds. Biomaterials 2003;24:3265–75.
[16] Kang JY, Chung CW, Sung JH, Park BS, Choi JY, Lee SJ, et al. Novel porous matrix of hyaluronic acid for the three-dimensional culture of chondrocytes. Int J Pharm 2009;369:114–20.
[17] Yamane S, Iwasaki N, Kasahara Y, Harada K, Majima T, Monde K, et al. Effect of pore size on in vitro cartilage formation using chitosan-based hyaluronic acid hybrid polymer fibers. J Biomed Mater Res A 2007;81:586–93.
[18] Komura M, Komura H, Kanamori Y, Tanaka Y, Suzuki K, Sugiyama M, et al. An animal model study for tissue-engineered trachea fabricated from a biodegradable scaffold using chondrocytes to augment repair of tracheal stenosis. J Pediatr Surg 2008;43:2141–6.
[19] Masuoka K, Asazuma T, Ishihara M, Sato M, Hattori H, Yoshihara Y, et al. Tissue engineering of articular cartilage using an allograft of cultured chondrocytes in a membrane-sealed atelocollagen honeycomb-shaped scaffold (ACHMS scaffold). J Biomed Mater Res B Appl Biomater 2005;75:177–84.
[20] Woodfield TB, Malda J, de Wijn J, Peters F, Riesle J, van Blitterswijk CA. Design of porous scaffolds for cartilage tissue engineering using a three-dimensional fiber-deposition technique. Biomaterials 2004;25:4149–61.
[21] Kang Y, Yang J, Khan S, Anissian L, Ameer GA. A new biodegradable polyester elastomer for cartilage tissue engineering. J Biomed Mater Res A 2006;77:331–9.
[22] Aoyagi R, Yoshida T. Freuqency equations of an ultrasonic vibrator for the elastic sensor using a contact impedance method. Jpn J Appl Phys 2004;5B: 3204–9.
[23] Miller RA, Brady JM, Cutright DE. Degradation rates of oral resorbable implants (polylactates and polyglycolates): rate modification with changes in PLA/PGA copolymer ratios. J Biomed Mater Res 1977;11:711–9.
[24] Matsusue Y, Yamamuro T, Oka M, Shikinami Y, Hyon SH, Ikada Y. In vitro and in vivo studies on bioabsorbable ultra-high-strength poly(L-lactide) rods. J Biomed Mater Res 1992;26:1553–67.
[25] Laitinen O, Tormala P, Taurio R, Skutnabb K, Saarelainen K, Iivonen T, et al. Mechanical properties of biodegradable ligament augmentation device of poly (L-lactide) in vitro and in vivo. Biomaterials 1992;13:1012–6.
[26] Wang Z, Wang S, Marois Y, Guidoin R, Zhang Z. Evaluation of biodegradable synthetic scaffold coated on arterial prostheses implanted in rat subcutaneous tissue. Biomaterials 2005;26:7387–401.
[27] Rich J, Kortesuo P, Ahola M, Yli-Urpo A, Kiesvaara J, Seppälä J. Effect of the molecular weight of poly(epsilon-caprolactone-co-DL-lactide) on toremifene citrate release from copolymer/silica xerogel composites. Int J Pharm 2001; 212:121–30.
[28] Takahashi T, Ogasawara T, Kishimoto J, Liu G, Asato H, Nakatsuka T, et al. Cell Transplant 2005;14:683–93.
[29] Tanaka Y, Ogasawara T, Asawa Y, Yamaoka H, Nishizawa S, Mori Y, et al. Growth factor contents of autologous human sera prepared by different production methods and their biological effects on chondrocytes. Cell Biol Int 2008;32: 505–14.
[30] Furukawa KS, Ushida T, Toita K, Sakai Y, Tateishi T. Hybrid of gel-cultured smooth muscle cells with PLLA sponge as a scaffold towards blood vessel regeneration. Cell Transplant 2002;11:475–80.
[31] Fujihara Y, Asawa Y, Takato T, Hoshi K. Tissue reactions to engineered cartilage based on poly-L-lactic acid scaffolds. Tissue Eng Part A 2009;15:1565–77.
[32] Klocke NW, Snyder PW, Widmer WR, Zhong W, McCabe GP, Breur GJ. Detection of synovial macrophages in the joint capsule of dogs with naturally occurring rupture of the cranial cruciate ligament. Am J Vet Res 2005;66:493–9.
[33] Smith MD, Triantafillou S, Parker A, Youssef PP, Coleman M. Synovial membrane inflammation and cytokine production in patients with early osteoarthritis. J Rheumatol 1997;24:365–71.
[34] Goldring MB. The role of the chondrocyte in osteoarthritis. Arthritis Rheum 2000;43:1916–26.
[35] Au RY, Al-Talib TK, Au AY, Phan PV, Frondoza CG. Avocado soybean unsaponifiables (ASU) suppress TNF-alpha, IL-1beta, COX-2, iNOS gene expression, and prostaglandin E(2) and nitric oxide production in articular chondrocytes and monocyte/macrophages. Osteoarthritis Cartilage 2007;15: 1249–55.
[36] Makino K, Ohshima H, Kondo T. Mechanism of hydrolytic degradation of poly (L-lactide) microcapsules: effects of pH, ionic strength and buffer concentration. J Microencapsul 1986;3:203–12.

TISSUE ENGINEERING: Part C
Volume 16, Number 6, 2010

DOI: 10.1089/ten.tec.2009.0597

The Optimal Conditions of Chondrocyte Isolation and Its Seeding in the Preparation for Cartilage Tissue Engineering

Kazumichi Yonenaga, D.D.S.,[1,2] Satoru Nishizawa, B.S.,[1] Yuko Fujihara, D.D.S., Ph.D.,[1] Yukiyo Asawa, D.V.M., Ph.D.,[1] Kanazawa Sanshiro, D.D.S.,[1] Satoru Nagata, M.D., Ph.D.,[3] Tsuyoshi Takato, M.D., Ph.D.,[2] and Kazuto Hoshi, M.D., Ph.D.[1]

To optimize the chondrocyte numbers obtained after collagenase digestion for cartilage tissue engineering, we examined the enzyme concentration and incubation time for collagenase digestion. The appropriate cell density in the chondrocyte primary culture was also verified. The collagenase digestion conditions that maximized the viable cell numbers were 24 h in 0.15% and 0.3% collagenase, 6 h in 0.6%, and 4 h in 1.2%, leading to $\sim 5\times10^5$ cells from 0.05 g. When seeded at 10,000 cells/cm^2, all of these cells became almost confluent within 1 week. Cells digested in 0.3% for 24 h or 0.6% for 6 h and seeded at 3000 cells/cm^2 may also be acceptable, and similarly reached confluence within 1 week. Results regarding expression of the p53, tumor necrosis factor-α, and interleukin-1β genes, as well as apoptosis enzyme-linked immunosorbent assay results, show that excessive collagenase exposure may decrease chondrocyte viability or activity. We recommend a 24-h incubation in 0.3% collagenase or 6 h in 0.6% collagenase, and a cell-seeding density of 3000–10,000 cells/cm^2. These conditions maximize the harvest of isolated chondrocytes from a small amount of biopsied tissue and significantly aid in obtaining a large quantity of cultured cells in a short period.

Introduction

In tissue engineering, cells are isolated from tissues/organs and cultured under biochemical and biophysical stimulation, eventually producing functionally equivalent tissues/organs. This procedure requires both a sufficient number of cells isolated from the tissues/organs and a high success rate of the primary culture. Although chondrocytes, which have been successful in various fields of regenerative medicine, are the major cell source for cartilage tissue engineering, they are difficult to isolate from cartilage because they contain abundant collagen-based matrices that require thorough digestion by collagenase.[1] Collagenase may decrease chondrocyte activity, not only because it damages the cell structure but also because chondrocytes separated from their native matrices show a decrease in proliferation, survival, and differentiation.[2] Because collagenase digestion might be a necessary evil during chondrocyte isolation, the concentration of collagenase and its incubation time should be restricted to a minimum. In previous reports, collagenase concentrations and incubation times during chondrocyte isolation varied widely (Table 1). The collagenase concentrations ranged from 0.03% to 0.6% (<1150 U/mL), and the incubation time ranged from 2 to 20 h.[3–30] Under these conditions, $\sim 1\times10^6$ cells/g of viable chondrocytes were harvested.[26] However, human cells are known to contain 1×10^8 cells/g,[31] which is 100 times more than the number of chondrocytes actually isolated. To increase the number of cells obtained after collagenase digestion, we attempted to determine the collagenase concentration and incubation time at which human chondrocytes are optimally digested.

The seeding density has a significant influence on cell viability and proliferation efficacy in the primary culture. If the seeding density is too low, the autocrine/paracrine system may barely work, which leads to slow proliferation. On the other hand, an overdose of chondrocytes may interfere with sufficient cell attachment to the substrate in the culture dish or evoke early contact inhibition, both of which lead to a less effective cell culture. However, the optimum seeding density in chondrocyte cultures for tissue engineering has not yet been investigated in detail. In this study, the appropriate cell density for the chondrocyte primary culture was also verified.

Materials and Methods

Chondrocyte isolation

All procedures were approved by the Ethics Committee of the University of Tokyo Hospital (ethics permission number

Departments of [1]Cartilage and Bone Regeneration (Fujisoft) and [2]Sensory and Motor System, Graduate School of Medicine, University of Tokyo, Tokyo, Japan.
[3]Nagata Microtia and Reconstructive Plastic Surgery Clinic, Saitama, Japan.

TABLE 1. COLLAGENASE CONCENTRATIONS FOR CHONDROCYTE ISOLATION IN PREVIOUS REPORTS

Collagenase concentration	*Unit (U/mL)*	*Time (h)*	*Collagenase subtype*	*Origin of cartilage*	*Digested cartilage*	*Reference*
0.6%	—	12	Type 2	Human	Nasal	3, 4
0.5%	1150	6–8	Normal	Human	Auricular	5
0.3%	690	4	Normal	Human	Auricular	6
0.3%	690	8–12	Normal	Human	Auricular	7
0.3%	690	8–12	Type 2	Human	Auricular	8–11
0.3%	690	12–18	Normal	Cow	Articular	12
0.25%	575	4–6	Normal	Human	Articular	13
0.2%	460	8	Type 2	Human	Auricular	14
0.2%	460	10–14	Type 2	Human	Nasal	15
0.2%	—	4	Type 2	Human	Articular	16
0.15%	291	Overnight	Normal	Human	Auricular	17–19
0.15%	—	Overnight	Type B	Rabbit	Auricular	20
0.1%	—	2	Type 1	Rabbit	Auricular	21
0.1%	—	3	Type A	Rabbit	Articular	22
0.1%	230	12	Type 2	Human	Nasal auricular	23
0.1%	230	14–16	Type 2	Pig	Nasal auricular Articular	24
0.1%	—	16	—	Human	Articular	25
0.08%	960	16–20	Normal	Human	Articular	26
0.07%	100	3	Type 2	Goat	Articular	27
0.04%	—	Overnight	—	Human	Articular	28
0.03%	—	12–18	Type P	Human	Nasal	29
0.03%	—	16	Type P	Human	Nasal	30

Dashes indicate lack of data.

622). Remnant auricular cartilage from three microtia patients was obtained during surgery in accordance with the Helsinki Principles. The cartilage tissue was thoroughly minced with scissors and tweezers into fragments of 250–1000 μm (Fig. 1A). Approximately 3 mL of collagenase solution (Wako Pure Chemical Industries) at concentrations of 0.15%, 0.3%, 0.6%, or 1.2% was poured into a 5 mL tube (BD Falcon). Four tubes were prepared for each concentration, for a total of 16 tubes. Approximately 0.05 g of cartilage fragments was put into each tube, which was then placed in a 37°C water bath and shaken at 150 cycles/min. For each concentration, the number of total cells and viable cells as well as the cell viability were measured with a Nucleo-Counter (ChemoMetec) after 2, 4, 6, and 24 h.

Chondrocyte culture

The viable cells were seeded in 6.4-mm plastic culture dishes coated with collagen type 1. Cells were seeded at densities of 30,000; 10,000; 3000; 1000; 300; and 100 cells/cm^2 for the evaluation of the optimal cell-seeding density for the primary culture. For the analysis of gene expression, 35-mm plastic culture dishes coated with collagen type 1 were used for the culturing of cells digested under certain conditions. The culture medium was Dulbecco's modified Eagle's medium Nutrient Mixture F-12 HAM (Sigma Chemical Co.) containing 5% human serum (Sigma Chemical Co.), 100 ng/mL fibroblast growth factor-2 (Kaken Pharmaceutical Co., Ltd.), and 5 μg/mL insulin (MP Biomedicals).[32]

Real-time reverse transcription (RT)-polymerase chain reaction analysis

Total RNA was isolated from the chondrocytes with ISOGEN (Wako Pure Chemical Industries) following the supplier's protocol. cDNA was synthesized from 1 μg of the total RNA with the PrimeScript® RT-PCR Kit Perfect Real Time (Takara Shuzo). The full-length or partial-length cDNA of the target genes, including the polymerase chain reaction (PCR) amplicon sequences, was amplified by PCR, cloned into pCR-TOPO Zero II or pCR-TOPO II vectors (Invitrogen), and used as standard templates after linearization. Using the QuantiTect SYBR Green PCR Master Mix (Invitrogen) and the ABI 7700 Sequence Detection System, we performed real-time fluorescence detection with the following protocol: initial denaturation for 10 min at 94°C followed by 40 cycles of 15 s at 94°C and 1 min at 60°C. All reactions were run in quadruplicate. The sequences of the primers were 5′-CCA GCCAAAGAAGAAACCAC-3′ and 5′-CTCATTCAGCTCTC GGAAC-3′ for p53, 5′-CCCCAGGGACCTCTCTCTAATC-3′ and 5′-GGTTTGCTACAACATGGGCTACA-3′ for tumor necrosis factor alpha (TNF-α), 5′-CCTGTCCTGCGTGTT GAAAGA-3′ and 5′-GGGAACTGGGCAGACTCAAA-3′ for interleukin 1beta (IL-1β), 5′-AGAACCTTGTGTGACAAAT GAGAAC-3′ and 5′-TACCCATTAGACATATCCAGCTT GA-3′ for bcl-2, and 5′-GAAGGTGAAGGTCGGAGTCA-3′ and 5′-GAAGATGGTGATGGGATTTC-3′ for glyceraldehyde-3-phosphate dehydrogenase.[33–36]

Photometry analysis of ssDNA apoptosis enzyme-linked immunosorbent assay

Five thousand cells were transferred into each well of a 96-well microplate, and the microplate was centrifuged at 200 *g* for 5 min. The medium was removed, and 200 μL of fixative (80% methanol in phosphate-buffered saline) was added to each microwell. The microplate was incubated at room temperature for 30 min, after which the fixative was removed, and the microplate was kept at room temperature for 1–2 h to

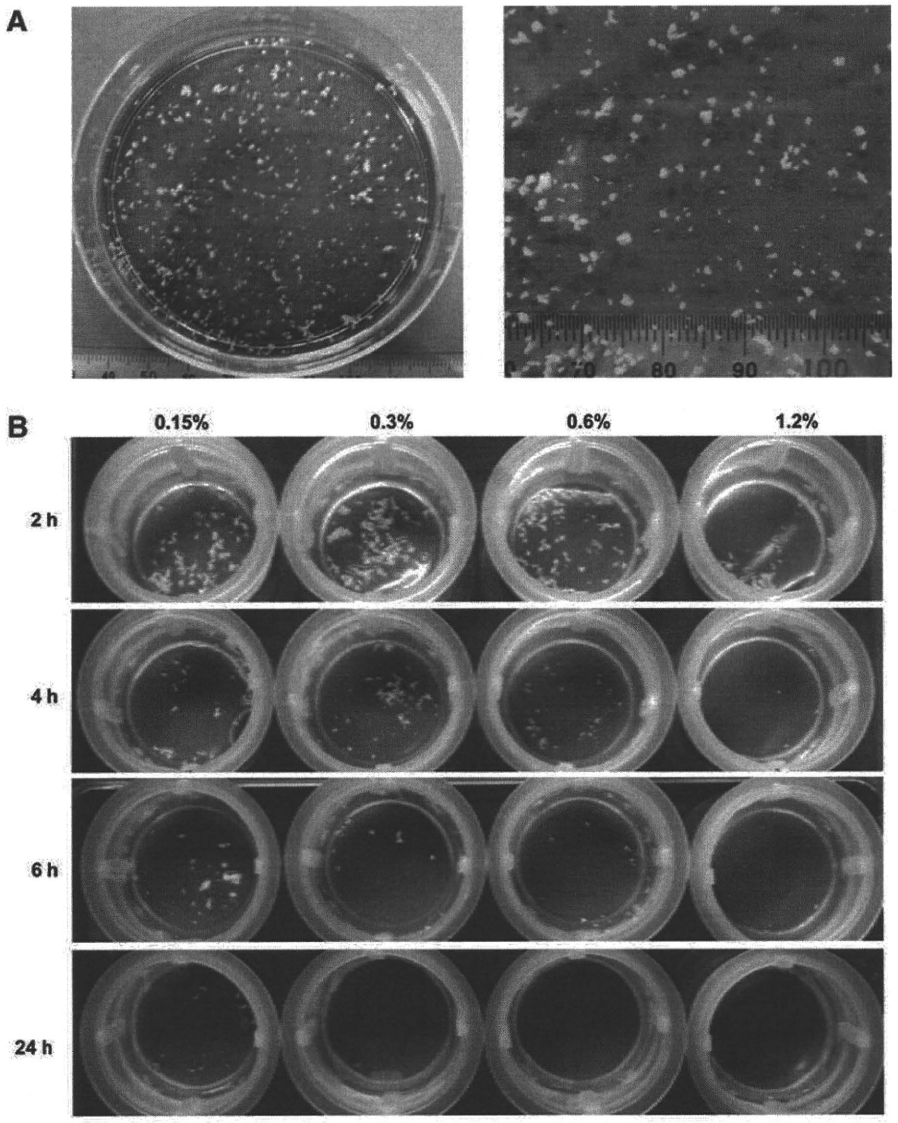

	0.15%	0.3%	0.6%	1.2%
2 h	+	+	+	±
4 h	+	+	±	-
6 h	+	±	-	-
24 h	±	-	-	-

FIG. 1. **(A)** Cartilage fragment after manual mincing. We measured the sizes of the fragments ($n = 100$) and determined them to be 643 ± 381 μm (mean ± standard deviation [SD]). This size and variation seemed almost average because the previous studies also reported fragment sizes of 250–1000[14] or 250–500 μm.[29,30] Left, higher magnification; right, lower magnification. **(B)** Collagenase digestion of the cartilage fragments. (Upper) At all concentrations, the sizes of the collagenase digests decreased as the incubation periods increased (2–24 h). (Lower) The chart shows the degree of cartilage digestion. Many fragments clearly remained (+); some fragments visible (±); all were digested (–).

allow attachment of the cells to the plate. Cell apoptosis was evaluated according to the manufacturer's protocol of the ssDNA Apoptosis ELISA Kit (Chemicon® International Inc.). The enzyme-linked immunosorbent assay absorbance was measured using a standard microplate reader at 405 nm.

Results

We examined the effects of collagenase concentration and incubation time on cartilage digestion. For all concentrations, the volume of the collagenase digests decreased as the incubation period increased (Fig. 1B). Although the cartilage pieces were somewhat visible after 24 h in the 0.15% collagenase, they had disappeared after the same amount of time in collagenase concentrations >0.3% (Fig. 1B). The amount of time for the cartilage remnants to disappear was shortened to 6 and 4 h in collagenase concentrations of 0.6% and 1.2%, respectively (Fig. 1B).

In all concentrations, both the total number of cells and the number of viable cells increased in parallel to the

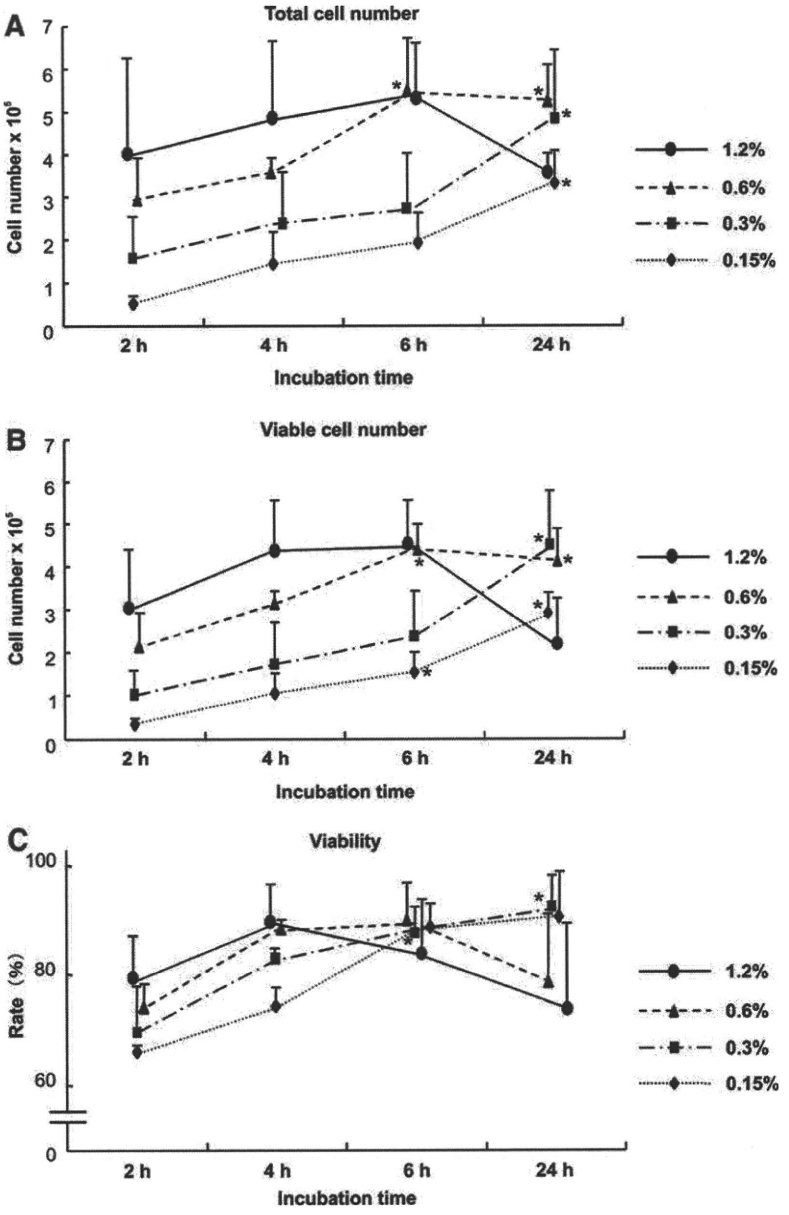

FIG. 2. Cell numbers and viability after collagenase digestion. Both the total **(A)** and viable **(B)** cell numbers increased with the increase in incubation time, except for the 1.2% collagenase. **(C)** Cell viability in 0.15% and 0.3% collagenase became ~100% at 24 h, whereas that in 0.6% collagenase reached maximum at 6 h. All values are presented as mean ± SD of three samples per group. Statistics were assessed using the Dunnett's test (*$p < 0.05$, vs. 2 h in each concentration of collagenase).

increase in the incubation time, with the exception of the sample with 1.2% collagenase for 24 h (Fig. 2A and B). The maximum number of viable cells, 4–5×10^5 cells obtained from ~0.05 g tissue, occurred at 4 h in 1.2% collagenase, 6 h in 0.6% collagenase, and 24 h in 0.3% collagenase. However, the sample with 0.15% collagenase provided <3×10^5 cells even after 24 h, possibly because of the abundant remnants of the cartilage digests (Fig. 2A and B). The total cell numbers and viable cell numbers under conditions of 24 h and 0.15% collagenase, 24 h and 0.3% collagenase, and 6 h and 0.6% collagenase were significantly higher than those at 2 h for each dose of collagenase (Fig. 2A and B). The cell numbers had decreased after 24 h in 1.2% collagenase, as the viability deteriorated (Fig. 2C). Therefore, we determined which conditions of collagenase digestion maximized the viable cell numbers and found that the incubation time can be reduced to 24 h in 0.15% collagenase and 0.3% collagenase, 6 h in 0.6% collagenase, and 4 h in 1.2% collagenase.

Next, we investigated the effect of cell density during seeding on cell growth (Fig. 3). Chondrocytes that had been digested by collagenase under suitable conditions as determined above were seeded at several cell densities (100–30,000 cells/cm^2). All of those seeded at 10,000 cells/cm^2 became almost confluent in 1 week. Seeding at 3000 cells/cm^2 may be acceptable for the chondrocytes digested with 0.3% collagen for 24 h and 0.6% for 6 h, but the cells digested under other conditions could not sufficiently proliferate at 3000 cells/cm^2 (Fig. 3B). The cells were aggregated with each other and formed cell clusters at 30,000 cells/cm^2 in the samples digested with 0.6% collagenase and 1.2% collagenase (Fig. 3A and B). When we counted the cell numbers, the cells seeded at a density of 3000–10,000 cells/cm^2 after di-

gestion in 0.3% collagenase for 24 h and 0.6% for 6 h reached the maximum cell numbers at 1 week (Fig. 4A), which supported the results shown in Figure 3. However, the cells seeded at <1000 cells/cm^2 became confluent as well after >2 weeks (Fig. 4B)

The possibility that the chondrocytes may fall into apoptosis or catabolic situations after the destruction of the native matrices by collagenase digestion could be not ignored. Thus, we examined gene expression of the apoptosis-related molecules and inflammatory cytokines in the chondrocytes for each set of collagenase digestion conditions. As shown in Figure 5, the proapoptotic factor p53 was likely upregulated as collagenase concentration increased, although we could not detect Bcl-2. The inflammatory cytokines TNF-α and IL-1β were scarcely detected in the chondrocytes digested in 0.15% collagenase for 24 h and in 0.3% collagenase for 24 h. Expression of these genes tended to increase in the chondrocytes with the higher collagenase concentrations (Fig. 5), suggesting that a collagenase concentration higher than 0.6% may somewhat affect chondrocyte viability or metabolism. Actually, the results of apoptosis assays also showed that apoptosis tended to be upregulated when the exposure time became longer in the higher concentrations of collagenase (0.6% or 1.2%). In contrast, the chondrocytes in the lower concentrations (0.15% and 0.3%) exhibited minimum apoptosis at 24 h (Fig. 6), which was consistent with the viability of chondrocytes (Fig. 2C) and the results of p53 expression (Fig. 5).

Discussion

Each laboratory engaged in the research and development of cartilage tissue engineering prepares various unique protocols according to their previous findings and experiences. Although they may independently work well, some kinds of standards are needed when we attempt to obtain stable results. However, thus far, no systematic analyses on collagenase

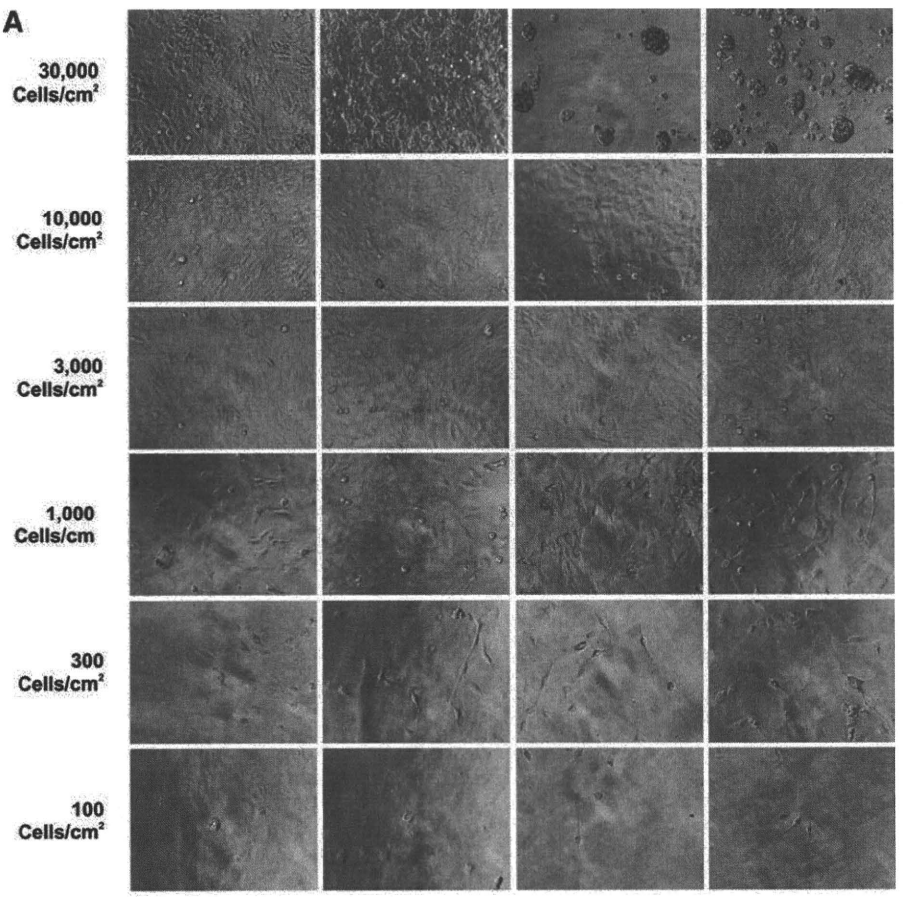

B

	0.15%/24h	0.3%/24h	0.6%/6h	1.2%/4h
30,000	○	○	×	×
10,000	○	○	○	○
3,000	○	○	○	○
1,000	△	△	△	△
300	△	△	△	△
100	△	△	△	△

FIG. 3. Optimal cell-seeding density to provide favorable cell growth. **(A)** The cells seeded at a density of 3000–10,000 cells/cm^2 became almost confluent in all the collagenase concentrations within 1 week. The cells at the density of <1000 cells/cm^2 could not sufficiently proliferate, whereas the cells tended to be aggregated at 30,000 cells/cm^2. **(B)** The chart shows the degree of cell growth. ○, confluent; Δ, did not reach confluence; ×, became aggregated.

doses or incubation times have been found. Although the cartilage includes different tissues and donor ages or diseases affect the cellularity or protein compositions of the tissues, the amount of collagen, which is the major inhibitory factor for chondrocyte isolation, seems almost constant.[37] This implies the possibility of a standard protocol. Thus, we regard the investigation of the optimal conditions for collagenase digestion to be a pivotal task for increasing the steadiness and safety of regenerative medicine.

On the basis of the results of the present study, by the time-course counting of cell numbers in various concentrations of collagenase, the maximum number of viable cells—5×10^5—were harvested from 0.05 g of original tissue at 24 h in 0.15% collagenase, 6 h in 0.6%, and 4 h in 1.2% (Fig. 2B). The incubation time at which the viable cell numbers reached a maximum corresponded to the point at which the collagenase digests completely disappeared (Fig. 1B). The reason why the harvested cell numbers in the 0.15% collagenase did not reach the maximum even at 24 h may be because the remaining cartilage digests in the solution at that time. The viability of the cells harvested at 2 h was lower than that of the later harvests. The cells harvested in this short incubation period had been located at the surface of the cartilage tissues that had been minced to $<1\,mm^3$ before the collagenase di-

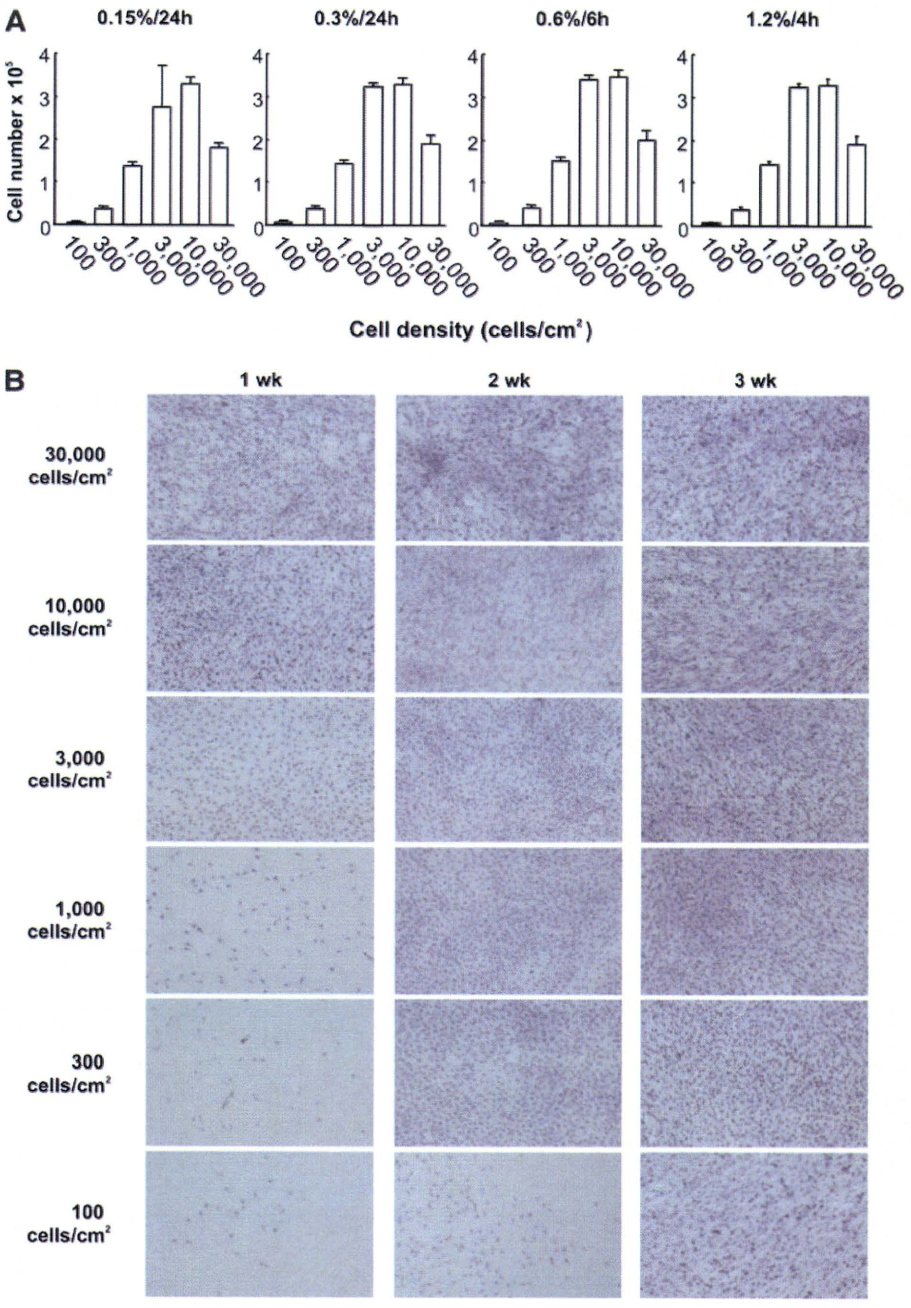

FIG. 4. Optimal cell-seeding density for obtaining sufficient cell numbers. **(A)** The cells seeded at a density of 3000–10,000 cells/cm^2 reached the maximum cell numbers at 1 week. All values are presented as mean ± SD of three samples per group. **(B)** The cells after digestion in 0.3% collagenase for 24 h were cultured for 3 weeks. They became confluent at >2 weeks when seeded at <1000 cells/cm^2. Color images available online at www.liebertonline.com/ten.

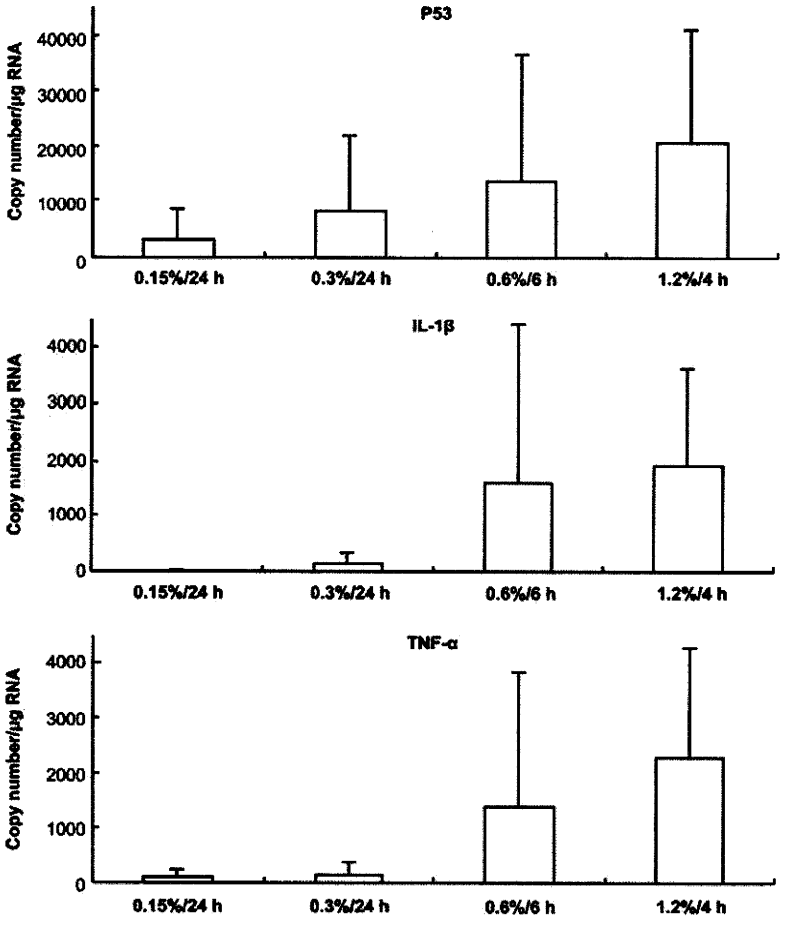

FIG. 5. Gene expression of the proapoptotic factor and the inflammatory cytokines. Gene expression of the proapoptotic factor, p53, or the inflammatory cytokines, tumor necrosis factor alpha (TNF-α), and interleukin 1beta (IL-1β) tended to be upregulated in the chondrocytes as the concentration of collagenase increased. All values are presented as mean ± SD of three samples per group.

gest. The mincing damaged the cells located on the surface of the tissues and decreased the viability of those cells. Therefore, the cells harvested after the 2 h incubation period showed a low viability (Fig. 2C). This tendency was also confirmed by the results of apoptosis assay. When the chondrocytes were exposed to lower concentrations of collagenase (0.15% or 0.3%), in which the cytotoxic effects of collagenase may hardly become obvious, those of short-term exposure (2–4 h) showed rather high extent of apoptosis (Fig. 6).

The cytotoxic effects of long-term exposure to collagenase were regarded as the cause of decrease in the viable cell numbers for those cells harvested at 24 h in 1.2% collagenase. In the present study, the maximum number of cells harvested from the native cartilage was $\sim 1\times10^7$ cells/g. These cell numbers were lower than those found in human cartilage (1×10^8 cells/g[31]), but it is a 10-fold increase when compared to previous data (1×10^6 cells/g[26]).

A cell density of 30,000 cells/cm^2 upon seeding was regarded as too high because the cells harvested from the

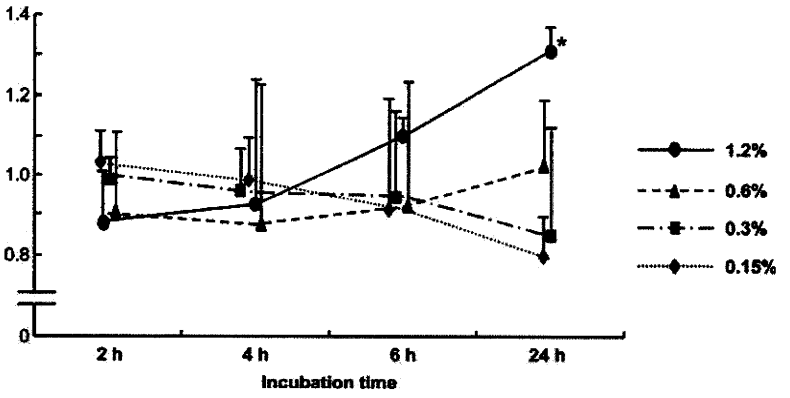

FIG. 6. Apoptosis enzyme-linked immunosorbent assay. Apoptosis appeared to be increased after digestion in 1.2% collagenase, especially at 24 h. All values are presented as mean ± SD of three samples per group. Statistics were assessed using the Dunnett's test (*$p < 0.05$, vs. 2 h in each concentration of collagenase).

0.6% to 1.2% collagenase digest tended to be aggregated, as seen in Figure 3. If fragments of the matrices remain around the chondrocytes after collagenase digestion, the chondrocytes may aggregate because cell aggregation is promoted by the matrix fragments that mediate the cell–matrix interaction.[38] Exposure to a higher concentration of collagenase even for a short incubation period could completely release the chondrocytes, but some fragments of the extracellular matrices may remain, which could mediate cell aggregation in a cell density as high as 30,000 cells/cm^2. In contrast, the density of 3000–10,000 cells/cm^2 showed appropriate adhesion and subsequent proliferation in all concentrations.

In addition, for a cell density lower than 1000 cells/cm^2, some viable cells were obtained after more than a week of incubation, as shown in Figure 4B.

It took 2 weeks for cells at initial densities <1000 cells/cm^2 to become confluent, and cells seeded at 100 cells/cm^2 needed as long as 3 weeks (Fig. 4B). However, if it takes >2 weeks for the chondrocytes to become confluent after seeding, too much time may be spent judging whether or not the chondrocytes have appropriately proliferated. A cell density at which the cells completely reach confluence within 1 week is desirable. Moreover, the paracrine/autocrine signals are needed for adequate cell proliferation.[39] Cells may not sufficiently proliferate at a low cell density because they cannot receive the paracrine/autocrine signals from adjacent cells. On the other hand, when the cell density is higher than 10,000 cells/cm^2, the passage would be needed at <1 week of incubation. If the incubation time during one passage is shortened and the passage number increases correspondingly, procedures become more complicated, and the risk of dedifferentiation may increase.

p53 and Bcl-2 are related to apoptosis. p53 induces apoptosis, participating in the maintenance of cell homeostasis.[33] Bcl-2, on the other hand, prohibits apoptosis.[34] TNF-α and IL-1β are inflammatory cytokines that are synthesized by natural immune cells in response to the infection or destruction of tissues.[35,36] Analysis of gene expression of these inflammatory cytokines, apoptosis-related molecules and apoptosis assay revealed that damage to the cells is diminished when the collagenase concentration is low. The damage to the cells may result from the cytotoxicity of the collagenase, which is a kind of digestive enzyme.

Therefore, we recommend a 24-h incubation in 0.3% collagenase, or 6 h in 0.6% collagenase, as the optimal condition for chondrocyte isolation from cartilage pieces that are 250–1000 μm in size. Moreover, the cell-seeding density should be in the range of 3000–10,000 cells/cm^2. These conditions maximize the harvest of the isolated chondrocytes from a small amount of biopsied tissue and significantly aid in obtaining a large quantity of cultured cells in a short period.

Acknowledgments

We thank Mr. Takashi Nakamoto, Ms. Miki Akizawa, Mr. Tomoaki Sakamoto, Mr. Takayuki Furuichi, and Mr. Makoto Watanabe for their technical support. This work was supported by Grants-in-Aid for Scientific Research from the Ministry of Education, Culture, Sports, Science and Technology of Japan (MEXT, No. 21390532 and 21659462), Research and Development Programs for Three-dimensional Complex Organ Structures from the New Energy and Industrial Technology Development Organization, and Resolving Critical Issues from Special Coordination Funds for Promoting Science and Technology (SCF) commissioned by MEXT.

Disclosure Statement

No competing financial interests exist.

References

1. Huckle, J., Dootson, G., Medcalf, N., McTaggart, S., Wright, E., Carter, A., Schreiber, R., Kirby, B., Dunkelman, N., Stevenson, S., Reiley, S., Davisson, T., and Ratcliffe, A. Differentiated chondrocytes for cartilage tissue engineering. Novartis Found Symp **249,** 103, 2003.
2. Asawa, Y., Ogasawara, T., Takahashi, T., Yamaoka, H., Nishizawa, S., Matsudaira, K., Mori, Y., Takato, T., and Hoshi, K. Aptitude of auricular and nasoseptal chondrocytes cultured under a monolayer or three-dimensional condition for cartilage tissue engineering. Tissue Eng Part A **15,** 1109, 2009.
3. Ruszymah, B.H.I., Lokman, B.S., Asma, A., Munirah, S., Chua, K., Mazlyzam, A.L., Isa, M.R., Fuzina, N.H., and Aminuddin, B.S. Pediatric auricular chondrocytes gene expression analysis in monolayer culture and engineered elastic cartilage. Int J Pediatr Otorhinolaryngol **71,** 1225, 2007.
4. Ruszymah, B.H.I., Chua, K.H., Mazlyzam, A.L., Fuzina, N.H., and Aminuddin, B.S. Formation of *in vivo* tissue-engineered human hyaline cartilage in the shape of a trachea with internal support. Int J Pediatr Otorhinolaryngol **69,** 1489, 2005.
5. Park, S.S., Jin, H.R., Chi, D.H., and Taylor, R.S. Characteristics of tissue-engineered cartilage from human auricular chondrocytes. Biomaterials **25,** 2363, 2004.
6. Yanaga, H., Yanaga, K., Imai, K., Koga, M., Soejima, C., and Ohmori, K. Clinical application of cultured autologous human auricular chondrocytes with autologous serum for craniofacial or nasal augmentation and repair. Plast Reconstr Surg **117,** 2019, 2006.
7. Rodriguez, A., Cao, Y.L., Ibarra, C., Pap, S., Vacanti, M., Eavey, R.D., and Vacanti, C.A. Characteristics of cartilage engineered from human pediatric auricular cartilage. Plast Reconstr Surg **103,** 1111, 1999.
8. Kamil, S.H., Woda, M., Bonassar, L.J., Novitsky, Y.W., Vacanti, C.A., Eavey, R.D., and Vacanti, M.P. Normal features of tissue-engineered auricular cartilage by flow cytometry and histology: patient safety. Otolaryngol Head Neck Surg **129,** 390, 2003.
9. Kamil, S.H., Rodrigruez, A., Vacanti, C.A., Eavey, R.D., and Vacanti, M.P. Expansion of the number of human auricular chondrocytes: recycling of culture media containing floating cells. Tissue Eng **10,** 139, 2004.
10. Kamil, S., Kojima, K., Vacanti, M., Zaporojan, V., Vacanti, C., and Eavey, R. Tissue-engineered cartilage: utilization of autologous serum and serum-free media for chondrocyte culture. Int J Pediatr Otorhinolaryngol **71,** 71, 2007.
11. Kamil, S.H., Vacanti, M.P., Vacanti, C.A., and Eavey, R.D. Microtia chondrocytes as a donor source for tissue-engineered cartilage. Laryngoscope **114,** 2187, 2004.
12. Cao, Y.L., Vacanti, J.P., Paige, K.T., *et al.* Transplantation of chondrocytes utilizing a polymer-cell construct to produce tissue-engineered cartilage in the shape of a human ear. Plast Reconstr Surg **100,** 297, 1997.

13. Ochi, M., Uchio, Y., Kawasaki, K., Wakitani, S., and Iwasa, J. Transplantation of cartilage-like tissue made by tissue engineering in the treatment of cartilage defects of the knee. J Bone Joint Surg Br **84,** 571, 2002.
14. Shieh, S.J., Terada, S., and Vacanti, J.P. Tissue engineering auricular reconstruction: *in vitro* and *in vivo* studies. Biomaterials **25,** 1545, 2002.
15. Rotter, N., Bonassar, L.J., Tobias, G., Lebl, M., Roy, A.K., and Vacanti, C.A. Age dependence of cellular properties of human septal cartilage: implications for tissue engineering. Arch Otolaryngol Head Neck Surg **127,** 1248, 2001.
16. Yoo, S.A., Park, B.H., Yoon, H.J., Lee, J.Y., Song, J.H., Kim, H.A., Cho, C.S., and Kim, W.U. Calcineurin modulates the catabolic and anabolic activity of chondrocytes and participates in the progression of experimental osteoarthritis. Arthritis Rheum **56,** 2299, 2007.
17. Liu, G., Kawaguchi, H., Ogasawara, T., Asawa, Y., Kishimoto, J., Takahashi, T., Chung, U.I., Yamaoka, H., Asato, H., Nakamura, K., Takato, T., and Hoshi, K. Optimal combination of soluble factors for tissue engineering of permanent cartilage from cultured human chondrocytes. J Biol Chem **282,** 20407, 2007.
18. Takahashi, T., Ogasawara, T., Asawa, Y., Mori, Y., Uchinuma, E., Takato, T., and Hoshi, K. Three-dimensional microenvironments retain chondrocyte phenotypes during proliferation culture. Tissue Eng **13,** 1583, 2007.
19. Yamaoka, H., Asato, H., Ogasawara, T., Nishizawa, S., Takahashi, T., Nakatsuka, T., Koshima, I., Nakamura, K., Kawaguchi, H., Chung, U.I., Takato, T., and Hoshi, K. Cartilage tissue engineering using human auricular chondrocytes embedded in different hydrogel materials. J Biomed Mater Res A **78,** 1, 2006.
20. Van Osch, G.J., Van der Veen, S.W., and Verwoerd-Verhoef, H.L. *In vitro* redifferentiation of culture-expanded rabbit and human auricular chondrocytes for cartilage reconstruction. Plast Reconstr Surg **107,** 433, 2001.
21. Moskalewski, S., and Thyberg, J. Reversible changes in nuclear and cell surface topography in cells exposed to collagenase and EDTA. Cell Tissue Res **220,** 51, 1981.
22. Brittberg, M., Nilsson, A., Lindahl, A., Ohlsson, C., and Peterson, L. Rabbit articular cartilage defects treated with autologous cultured chondrocytes. Clin Orthop **326,** 270, 1996.
23. Naumann, A., Dennis, J.E., Aigner, J., Coticchia, J., Arnold, J., Berghaus, A., Kastenbauer, E.R., and Caplan, A.I. Tissue engineering of autologous cartilage grafts in three-dimensional *in vitro* macroaggregate culture system. Tissue Eng **10,** 1695, 2004.
24. Johnson, T.S., Xu, J.W., Zaporojan, V.V., Mesa, J.M., Weinand, C., Randolph, M.A., Bonassar, L.J., Winograd, J.M., and Yaremchuk, M.J. Integrative repair of cartilage with articular and nonarticular chondrocytes. Tissue Eng **10,** 1308, 2004.
25. Brittberg, M., Lindahl, A., Nilsson, A., Ohlsson, C., Isaksson, O., and Peterson, L. Treatment of deep cartilage defects in the knee with autologous chondrocyte transplantation. N Engl J Med **331,** 889, 1994.
26. Peterson, L., Minas, T., Brittberg, M., *et al.* Two- to 9-year outcome after autologous chondrocyte transplantation of the knee. Clin Orthop **374,** 212, 2000.
27. Hayes, A.J., Hall, A., Brown, L., Tubo, R., and Caterson, B. Macromolecular organization and *in vitro* growth characteristics of scaffold-free neocartilage grafts. J Histochem Cytochem **55,** 853, 2007.
28. Melero-Martin, J.M., Dowling, M.-A., Smith, M., and Al-Rubeai, M. Expansion of chondroprogenitor cells on macroporous microcarriers as an alternative to conventional monolayer systems. Biomaterials **27,** 2970, 2006.
29. Chia, S., Homicz, M., Schumacher, B., Thonar, E., Masuda, K., Sah, R., *et al.* Characterization of human nasal septal chondrocytes cultured in alginate. J Am Coll Surg **200,** 691, 2005.
30. Alexander, T., Sage, A., Schumacher, B., Sah, R., and Watson, D. Human serum for tissue engineering of human nasal septal cartilage. Otolaryngol Head Neck Surg **135,** 397, 2006.
31. Bassermann, F., Frescas, D., Guardavaccaro, D., Busino, L., Peschiaroli, A., and Pagano, M. The Cdc14B-Cdh1-Plk1 axis controls the G2 DNA-damage-response checkpoint. Cell **134,** 256, 2008.
32. Tanaka, Y., Ogasawara, T., Asawa, Y., Yamaoka, H., Nishizawa, S., Mori, Y., Takato, T., and Hoshi, K. Growth factor contents of autologous human sera prepared by different production methods and their biological effects on chondrocytes. Cell Biol Int **32,** 505, 2008.
33. Oda, K., Arakawa, H., Tanaka, T., Matsuda, K., Tanikawa, C., Mori, T., Nishimori, H., Tamai, K., Tokino, T., Nakamura, Y., and Taya, Y. p53AIP1, a potential mediator of p53-dependent apoptosis, and its regulation by Ser-46-phosphorylated p53. Cell **102,** 849, 2000.
34. Kinnally, K.W., and Antonsson, B. A tale of two mitochondrial channels, MAC and PTP, in apoptosis. Apoptosis **12,** 857, 2007.
35. Locksley, R.M., Killeen, N., and Lenardo, M.J. The TNF and TNF receptor superfamilies: integrating mammalian biology. Cell **104,** 487, 2001.
36. Morgan, M.M., Clayton, C.C., and Heinricher, M.M. Dissociation of hyperalgesia from fever following intracerebroventricular administration of interleukin-1beta in the rat. Brain Res **1022,** 96, 2004.
37. Ross, M.H., Romrell, L.J., and Kaye, G.I. Histology: A Text and Atlas, 3rd edition. Baltimore, MD: Williams & Wilkins, 1995.
38. Steck, E., Br Bun, J., Pelttari, K., Kadel, S., Kalbacher, H., and Richter, W. Chondrocyte secreted CRTAC1: a glycosylated extracellular matrix molecule of human articular cartilage. Matrix Biol **26,** 30, 2007.
39. Olney, R.C., Wang, J., Sylvester, J.E., and Mougey, E.B. Growth factor regulation of human growth plate chondrocyte proliferation *in vitro*. Biochem Biophys Res Commun **317,** 1171, 2004.

Address correspondence to:
Kazuto Hoshi, M.D., Ph.D.
Department of Cartilage and Bone Regeneration (Fujisoft)
Graduate School of Medicine
University of Tokyo
Hongo 7-3-1, Bunkyo-ku
Tokyo 113-8655
Japan

E-mail: pochi-tky@umin.net

Received: September 4, 2009
Accepted: April 20, 2010
Online Publication Date: October 28, 2010

Biomaterials 31 (2010) 8004–8011

Contents lists available at ScienceDirect

Biomaterials

journal homepage: www.elsevier.com/locate/biomaterials

The influence of skeletal maturity on allogenic synovial mesenchymal stem cell-based repair of cartilage in a large animal model

Kazunori Shimomura [a], Wataru Ando [a], Kosuke Tateishi [a], Ryosuke Nansai [b], Hiromichi Fujie [b], David A. Hart [c], Hideyuki Kohda [a], Keisuke Kita [a], Takashi Kanamoto [a], Tatsuo Mae [a], Ken Nakata [a], Konsei Shino [d], Hideki Yoshikawa [a], Norimasa Nakamura [e,f,*]

[a] Department of Orthopaedics, Osaka University Graduate School of Medicine, 2-2 Yamadaoka, Suita City, Osaka 565-0871, Japan
[b] Biomechanics Laboratory, Department of Mechanical Engineering, Kogakuin University, 2665-1 Nakanomachi, Hachioji City, Tokyo 192-0015, Japan
[c] McCaig Institute for Bone & Joint Health, University of Calgary, 3330 Hospital Drive Northwest, Calgary, Alberta T2N 4N1, Canada
[d] Faculty of Comprehensive Rehabilitation, Osaka Prefecture University, 3-7-30 Habikino, Habikino City, Osaka 583-8555, Japan
[e] Department of Rehabilitation Science, Osaka Health Science University, 1-9-27 Tenma, Kita-ku, Osaka City, Osaka 530-0043, Japan
[f] Center for Advanced Medical Engineering and Informatics, Osaka University, 2-2 Yamadaoka, Suita City, Osaka 565-0871, Japan

ARTICLE INFO

Article history:
Received 23 May 2010
Accepted 4 July 2010
Available online 31 July 2010

Keywords:
Mesenchymal stem cell
Cartilage tissue engineering
Allogenic cell
Aging
Animal model

ABSTRACT

One of the potential factors that may affect the results of mesenchymal stem cell (MSC)-based therapy is the age of donors and recipients. However, there have been no controlled studies to investigate the influence of skeletal maturity on the MSC-based repair of cartilage. The purpose of this study was to compare the repair quality of damaged articular cartilage treated by a scaffold-free three-dimensional tissue-engineered construct (TEC) derived from synovial MSCs between immature and mature pigs. Synovial MSCs were isolated from immature and mature pigs and the proliferation and chondrogenic differentiation capacities were compared. The TEC derived from the synovial MSCs were then implanted into equivalent chondral defects in the medial femoral condyle of both immature and mature pigs, respectively. The implanted defects were morphologically and biomechanically evaluated at 6 months postoperatively. There was no skeletal maturity-dependent difference in proliferation or chondrogenic differentiation capacity of the porcine synovial MSCs. The TEC derived from synovial MSCs promoted the repair of chondral lesion in both immature and mature pigs without the evidence of immune reaction. The repaired tissue by the TEC also exhibited similar viscoelastic properties to normal cartilage regardless of the skeletal maturity. The results of the present study not only suggest the feasibility of allogenic MSC-based cartilage repair over generations but also may validate the use of immature porcine model as clinically relevant to test the feasibility of synovial MSC-based therapies in chondral lesions.

1. Introduction

It is widely accepted that chondral injury does not usually heal spontaneously due to its avascular surroundings and unique matrix organization. Therefore, a variety of approaches have been assessed to improve cartilage healing [1,2]. Among them, chondrocyte-based therapies have been extensively studied since the reports of successful autologous chondrocyte implantation [3–8]. However, this procedure is likely to have some limitations including the sacrifice of undamaged cartilage within the same joint and alterations of chondrogenic phenotype associated with the *in vitro* expansion of the cells. Furthermore, due to alterations and degenerative changes in cartilage accompanying aging, the availability of such cells may be limited in elderly individuals [7,9].

To overcome such potential problems, stem cell therapies have been tested to facilitate regenerative tissue repair. Mesenchymal stem cells (MSCs) have the capability to differentiate into a variety of connective tissue cells including bone, cartilage, tendon, muscle, and adipose tissue [10]. These cells may be isolated from various tissues such as bone marrow, skeletal muscle, synovial membrane, adipose tissue, and umbilical cord blood [10–15]. MSCs isolated from synovial membrane may be well suited for cell-based therapies for cartilage based on the relative ease of their harvest and their strong capability of chondrogenic differentiation [11,14,16]. Recent implantation studies have reported successful cartilage repair using synovial membrane-derived MSCs [12,15,17].

* Corresponding author. Department of Rehabilitation Science, Osaka Health Science University, 1-9-27 Tenma, Kita-ku, Osaka City, Osaka 530-0043, Japan. Tel.: +81 6 6352 0093; fax: +81 6 6352 9559.
E-mail address: n-nakamura@ort.med.osaka-u.ac.jp (N. Nakamura).

0142-9612/$ – see front matter © 2010 Elsevier Ltd. All rights reserved.
doi:10.1016/j.biomaterials.2010.07.017

One of the crucial factors that may affect the results of cell-based therapies is the age of the donors and recipients. Specifically, the results of implantation surgery could be potentially affected by both the characteristics of the cells and the local environment in the lesions following implantation. Therefore, it is important to elucidate the influence of skeletal maturity on these two factors. Regarding the cell proliferation and differentiation capacities of MSCs, it is controversial as to whether they are age-dependent [18–21] or not [10,22–25]. In terms of the host tissue reaction, natural healing responses of osteochondral defects has been compared between immature and mature animals using rabbit models, and in this species the studies demonstrated better healing responses in immature animals [26–29].

On the other hand, there have been no studies which compared the results of cell-based repair of chondral defects between immature and mature animal models. Regarding the clinically relevant animal models for cartilage repair, it is difficult to create a chondral injury which does not breach the subchondral bone in small animals such as rabbits, rats and mice due to the limited thickness of their articular cartilage. Therefore, in consideration of clinical relevance, it is preferable to utilize a large animal model to investigate the influence of maturity on the results of cell-based therapy in chondral lesions.

As a potential MSC-based therapeutic method, we have developed a scaffold-free three-dimensional tissue-engineered construct (TEC) composed of allogenic mesenchymal stem cells (MSCs) derived from the synovium and extracellular matrices (ECMs) synthesized by the cells [11], and demonstrated the feasibility of the resultant TEC to facilitate cartilage repair in a large animal study [12]. The TEC efficiently repaired the chondral defects by developing a cartilage-like tissue without the development of any immunologic reaction [12]. A potential limitation of this previous study was the use of an immature animal model (cell donors and recipients) and a concern that the successful chondrogenic repair without immunologic reaction *in vivo* might have been due to the immaturity of the recipient animals which may be a growth-oriented environment.

In the present study, we used both skeletally immature and mature animals as recipients, and compared the results of TEC implantation to the chondral lesions morphologically and biomechanically in order to elucidate the influence of the skeletally maturity on subsequent cartilage repair with the TEC.

2. Materials and methods

All procedures of this study followed the Declaration of Helsinki principles.

2.1. Harvest of synovial tissue and isolation of the cells

Porcine synovial membranes were obtained aseptically from the knee joints of immature (3–4 months of age) ($N = 3$) or mature (12 months of age) ($N = 3$) male pigs within 12 h of death. The cell isolation protocol was essentially that used previously for the isolation of human synovial derived MSC [11]. Briefly, synovial membrane specimens were rinsed with phosphate buffered saline (PBS), minced meticulously, and digested with 0.1% collagenase IV (Sigma, St. Louis, MO, USA) for 1.5 h at 37 °C. After neutralization of the collagenase with growth medium containing high-glucose Dulbecco's modified Eagle's medium (HG-DMEM; Gibco BRL, Life Technologies Inc., Rockville, MD, USA) supplemented with 10% fetal bovine serum (FBS; HyClone, Logan, UT, USA) and 1% penicillin/streptomycin (Gibco BRL, Life Technologies Inc.), the cells were collected by centrifugation, washed with PBS, resuspended in growth medium, and plated in culture dishes. The characteristics of the porcine cells were similar to those of the human synovium derived MSC with regard to morphology, growth characteristics and multipotent differentiation capacity (to osteogenic, chondrogenic and adipogenic lineages) [11,12,30]. For expansion, cells were cultured in the growth medium at 37 °C in a humidified atmosphere of 5% CO_2. The medium was replaced once per week. After 15–28 days of primary culture, when the cells reached confluence, they were washed twice with PBS, harvested by treatment with trypsin-EDTA (0.25% trypsin and 1 mM EDTA: Gibco BRL, Life Technologies Inc.), and replated at 1:3 dilutions for the first subculture. Cell passages were continued in the same manner with 1:3 dilutions when cultures reached near confluence. Cells at passages 4–7 were used in the present studies.

2.2. Cell proliferation assay

To assess cell proliferation between cells derived from immature and mature animals, cell counts and WST-1 assays [31,32] were performed at day 1, 3, 7, 10 and 14 of culture. The cells were isolated by trypsinization, washed extensively, and then replated at a density of 5×10^3 cells/cm^2 in 6-well and 96-well culture plates for cell counts and WST-1 assays, respectively. MSCs were cultured in growth medium and the medium was replaced twice per week. Subsequently, the numbers of cells were counted at each measurement day using a hemocytometer. In addition, 10 μl of Premix WST-1 solution (TAKARA Bio, Shiga, Japan) and 100 μl of medium were added to the cell monolayers in the 96-well plates and these were then incubated at 37 °C for an additional 2 h. Supernatants were quantified spectrophotometrically at 440 nm with reference wavelength at 620 nm. Results were reported as optical density (OD) units.

2.3. In vitro chondrogenesis

To assess chondrogenic differentiation, a pellet culture system was used [33]. Approximately 2×10^5 cells were placed in a 15-ml polypropylene tube, and centrifuged at 500 g for 10 min. The pellets were cultured at 37 °C with 5% CO_2 in 500 μl of chondrogenic culture medium that contained HG-DMEM supplemented with 50 mg/ml ascorbate-2-phosphate, 100 mg/ml sodium pyruvate, and 50 mg/ml insulin, transferrin, selenious acid (ITS) + Premix (BD Biosciences, California, USA), and 200 ng/ml recombinant human bone morphogenetic protein 2 (rhBMP2) (a generous gift from Wyeth, Massachusetts, USA) as described previously [30,34]. The optimal concentration of rhBMP2 was determined from preliminary *in vitro* optimization studies on chondrogenic differentiation of MSCs in pellet cultures (data not shown). The medium was replaced twice per week for 3 weeks.

2.4. Reverse transcription-polymerase chain reaction (RT-PCR)

Total RNAs from the pellets were extracted using a RNeasy Mini Kit (Qiagen, Valencia, CA, USA). Complementary DNAs (cDNAs) were obtained by RT of 1 μg total RNA using a Reverse Transcription System (Promega, San Luis Obispo, CA, USA) with random primers. Equal amounts of each RT product were amplified by PCR with TaKaRa Ex Taq (TAKARA Bio, Shiga, Japan). PCR reactions were carried out in iCycler™ (BioRad Laboratories, Hercules, CA, USA). After initial denaturation at 94 °C for 5 min, PCR involved amplification cycles of 30 s at 94 °C, 30 s at 60 °C, and 30 s at 72 °C, followed by elongation for 7 min at 72 °C. PCR primers used were as follows: pig-GAPDH (forward): CTG CCC CTT CTG CTG ATG C, (reverse): CAT CAC GCC ACA GTT TCC CA, pig-collagen 2a1 (forward): ATT GTA GGA CCC AAA GGA CCT C, (reverse): GGT CCC AGG TTC TCC ATC TC. PCR products were separated on 2% agarose gel containing ethidium bromide and evaluated for the expression of mRNA for each gene. The band intensities were captured into a computer with a digital image scanner, quantified using imageJ (NIH, Bethesda, MD) and subjected to statistical analyses.

2.5. Histological assessment of the pellets

The cell pellet cultures were fixed in 4% paraformaldehyde, rinsed twice with PBS, embedded in paraffin, cut into 5 μm sections, and then stained for 2 h at room temperature with 1% Alcian blue (Alcian Blue 8 GX; Sigma, Missouri, USA) in 0.1N HCl, and subsequently counter stained with Kernechtrot.

2.6. Measurement of glycosaminoglycan (GAG) levels

Proteoglycan levels in the pellets were measured by a color method as described previously [35], with minor modification. Briefly, synovial cell pellets were digested for 4 h at 65 °C with a papain solution (Sigma, St. Louis, MO, USA). Samples from the papain digest were subsequently assayed for GAG as a measure of proteoglycan content. GAGs were assayed using the 1,9-dimethylmethylene blue binding (DMMB) assay, using a chondroitin sulfate standard curve (Nacalai Tesque, Kyoto, Japan).

2.7. Development of the TECs

Synovial MSCs were plated on culture dishes at a density of 4.0×10^5 cells/cm^2 in growth medium containing 0.2 mM ascorbate-2-phosphate (Asc-2P), an optimal concentration from earlier studies [11,12]. Within a day, the cells became confluent. After an additional 7–14 days in culture, a complex of the cultured cells and the ECM synthesized by the cells was detached from the substratum by application of shear stress using gentle pipetting. The detached monolayer complex was left in suspension to form a three-dimensional structure by active tissue contraction. This tissue was termed a basic scaffold-free three-dimensional TEC.

2.8. Implantation of the TEC to chondral defects

As previously reported [12], porcine MSCs (4.0×10^5 cells/cm^2) derived from immature animals (3–4 months of age) were cultured with Asc-2P in 6 cm